

Fall 11-2015

Development and Prototype Validation of an Additive Manufactured Cubesat Propulsion Tank

Geovanni A. Solorzano
Embry-Riddle Aeronautical University

Follow this and additional works at: <https://commons.erau.edu/edt>



Part of the [Mechanical Engineering Commons](#)

Scholarly Commons Citation

Solorzano, Geovanni A., "Development and Prototype Validation of an Additive Manufactured Cubesat Propulsion Tank" (2015). *Doctoral Dissertations and Master's Theses*. 249.
<https://commons.erau.edu/edt/249>

This Thesis - Open Access is brought to you for free and open access by Scholarly Commons. It has been accepted for inclusion in Doctoral Dissertations and Master's Theses by an authorized administrator of Scholarly Commons. For more information, please contact commons@erau.edu.

DEVELOPMENT AND PROTOTYPE VALIDATION OF AN ADDITIVE
MANUFACTURED CUBESAT PROPULSION TANK

by

Geovanni A. Solorzano

A Thesis Submitted to College of Engineering Department of Mechanical
Engineering in Partial Fulfillment for the Requirements for the Degree of Master
of Science in Mechanical Engineering

Embry-Riddle Aeronautical University
Daytona Beach, Florida
December 2015

DEVELOPMENT AND PROTOTYPE VALIDATION OF AN ADDITIVE
MANUFACTURED CUBESAT PROPULSION TANK

by

Geovanni A. Solorzano

This thesis was prepared under the direction of the candidate's Thesis Committee Chair,
Dr. Bogdan Udrea, Professor, Daytona Beach Campus, and Thesis Committee Members

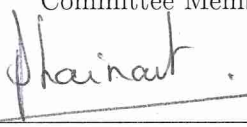
Dr. Heidi M. Steinhauer, Professor, Daytona Beach Campus, and Dr. Sathya
Gangadharan, Professor, Daytona Beach Campus, and has been approved by the Thesis
Committee. It was submitted to the Department of Mechanical Engineering in partial
fulfillment of the requirements for the degree of Master of Science in Mechanical
Engineering

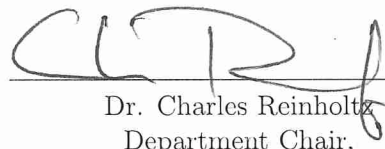
Thesis Review Committee:




Dr. Bogdan Udrea
Committee Chair

Dr. Heidi M. Steinhauer
Committee Member

Dr. Sathya Gangadharan
Committee Member

Dr. Jean-Michel Dhainaut
Graduate Program Chair,
Mechanical Engineering

Dr. Charles Reinholtz
Department Chair,
Mechanical Engineering

Dr. Maj Mirmirani,
Dean, College of Engineering

Dr. Christopher Grant,
Associate Vice President of Academics

Acknowledgements

First and foremost I wish to thank my advisor, Dr. Bogdan Udrea. He has been supportive since the days I began working on Project ARAPAIMA as an undergraduate; I remember he used to say something like "we're going to do real work and treat this like a company unlike other classes" to encourage me to stay in the lab and Project ARAPAIMA. Ever since, Dr. Bogdan Udrea has supported me not only by providing a research assistantship through the NASA Florida Space Grant Consortium and the Air Force UNP for almost three years, but also academically through the rough road to finish this thesis. Thanks to him I had the opportunity to design and build ARAPAIMA's propulsion tank and test it till failure! He helped me come up with the thesis topic and guided me over almost a year of development. And during the most difficult times when writing this thesis, he gave me the moral support and the freedom I needed to move on.

I would also like to thank Dr. Heidi M. Steinhauer, and Dr. Sathya Gangadharan for guiding my research for the past several years and helping me to develop my background in CAD design, additive manufacturing, structural optimization, and design for manufacturing and assembly. I will forever be thankful to ARAPAIMA's co-investigator, Dr. Adam Huang from the University of Arkansas. Dr. Huang has been helpful in providing the project with his cubesat research and ideas. Without his research focus in miniaturization sciences for aerospace systems, pico/nano-satellites and micro-propulsion system, none of this would have reached the age of maturity it is now. I greatly appreciate the financial support from AFOSR, AFRL, and NASA Florida Space Grant Consortium that funded parts of the research discussed in this thesis.

My time at "Riddle" was made enjoyable in large part due to the many friends and groups that became a part of my life. I am grateful for time spent with roommates and friends, for my climbing buddies and our memorable trips going to the climbing gym, for Rachelle Sarnow and Samantha Hurths's hospitality while at the fitness gym as I finished up my degree, and for many other people and memories.

I would also like to thank Jordan Beckwith for helping me prepare the propulsion tank for testing and sharing her manufacturing and machining expertise. This includes but not limited to drill and tap, welding, and many golden nuggets of advice. Without Mike Potash, my soldering would have wasted all the strain gages that were purchased. He was also kind enough to lend me the strain gage quarter bridge/amplifier and bipolar power supply.

Finally, I take this opportunity to express the profound gratitude from my deep heart to my beloved parents, grandparents, and my sibling for their love and contin-

uous support – both spiritually and materially. Without your support and drive for me to succeed and get out of Compton,CA, none of this would have been possible. *Me eche las pilas* and I wholeheartedly thank you.

Abstract

Author: Geovanni A. Solorzano
Title: Development and Prototype Validation of an Additive
 Manufactured Cubesat Propulsion Tank
Institution: Embry-Riddle Aeronautical University
Degree: Master of Science in Mechanical Engineering
Year: 2015

The purpose of this study is to determine if a cubesat propellant tank using the additive manufacturing technology of direct metal laser sintering meets the requirements, and material properties of a conventionally manufactured tank. Additionally, to see if additive manufactured parts are a viable option to be used in cubesat applications. This was accomplished by designing a model which will be used by the ARAPAIMA cubesat that meets all the Air Force's University Nanosatellite Program (UNP), NASA's and Department of Defense's requirements for pressurized vessels and material properties. A finite element analysis study was conducted to determine where and when the propulsion tank will fail using an isotropic material. Afterwards two propulsion tanks were manufactured, one for nondestructive evaluation and inspection and the other for destructive testing. The tank for destructive testing was prepared for hydrostatic pressure test, by plugging the holes for external components and by installing six strain gages. The purpose of the test has been to compare the material properties of the isotropic FEA model of the tank to the anisotropic 3D printed tank.

After testing the propulsion tank to failure in the hydrostatic pressure chamber, it is clear that the AlSi10Mg material is stronger than a billet Aluminum 6061 T-6. The maximum operating pressure of the propulsion tank is 160 psi and the pressure the tank ruptured is 410psi proves that FEA correctly predicted a factor of safety of 2.10. The results also proved that the propulsion tank was over designed and needs to be optimized to reduce weight and be redesigned for additive manufacturing in mind, such as an internal lattice support structure. Some features are still included to ease the labor if manufactured by conventional means.

Contents

Signature Page	i
Acknowledgements	ii
Abstract	iv
List of Figures	viii
List of Tables	viii
1 Introduction	1
1.1 Significance of the Study	1
1.2 Purpose Statement	2
1.3 UNP Constraints	2
1.4 Limitations and Assumptions	2
2 Review of the Relevant Literature	4
2.1 CubeSat Overview	4
2.1.1 CubeSat Propulsion	6
2.2 ARAPAIMA CubeSat	8
2.2.1 ARAPAIMA's Propulsion Subsystem	9
2.3 Additive Manufacturing Overview	12
2.3.1 Powder Bed Fusion Processes	13
2.4 Hypothesis	14
3 Methodology	15
3.1 Research Approach	15
3.1.1 Tank Design	15
3.1.1.1 Size Constraints	15
3.1.1.2 Material Constraints	17

3.2	Propellant Tank Modifications	19
3.2.1	Design Modifications for AM	19
3.2.1.1	Build Orientation	20
3.2.1.2	Bosses, Gussets, and Hole Diameters	21
3.2.2	Hardware Modifications for Testing	22
3.3	FEA Study	23
3.4	Experiment Testing Equipment	25
3.4.1	Hydrostatic Pressure Test System	25
3.4.2	Strain Gage	26
3.4.3	Pressure Transducer	29
3.4.4	Data Acquisition Cards	30
3.4.5	LabVIEW	30
4	Results	34
4.1	Additive Manufacturing Results	34
4.2	FEA Results	36
4.3	Propellant Tank Hydrostatic Pressure Test Results	36
5	Discussion, Conclusion & Recommendations	39
5.1	Discussion	39
5.2	Conclusion	42
5.3	Recommendations and Future Work	42
5.4	Application	43
	References	45
	Appendix A Propulsion Tank Detailed Drawings	46
	Appendix B EOS Aluminium AlSi10Mg Data Sheet	51
	Appendix C SEM Material Test Sample Results	57

List of Figures

2.1	Different configurations of cubesats ranging from 1U to 3U [12]	5
2.2	Newer and larger proposed cubesat sizes [4]	6
2.3	Popular cubesat deployers	6
2.4	Cold-Gas propulsion system schematic [23]	7
2.5	CAD model of the ARAPAIMA cubesat	8
2.6	ARAPAIMA's Propulsion Fluidic System Diagram	10
2.7	ARAPAIMA's Detailed Propulsion System	11
2.8	Generic schematic of an AM powder bed fusion system [9]	13
3.1	2U of space available for propulsion subsystem	16
3.2	Design iterations of the propulsion subsystem	16
3.3	ARAPAIMA cubesat fit check	17
3.4	2U of space available for propulsion subsystem	17
3.5	Recommend design modifications for the AM process	20
3.6	Self supporting angles of 316L Stainless steel with 30 micron layers [18]	21
3.7	Build Orientation with support structure	21
3.8	Bosses increased to accommodate the AM process	22
3.9	Harnessing holes that will be removed to be precisely machined later	22
3.10	Drilled and tapped holes for testing	23
3.11	Before and after of the front four holes	23
3.12	Propellant tank features removed for mesh generation	24
3.13	Fixed support applied to the hardware interface holes	24
3.14	160 psi of outward pressure applied to the surface	25
3.15	Hydrostatic Chamber Schematic and physical system	26
3.16	Basic Wheatstone Bridge Circuit Diagram [14]	27
3.17	Purchased strain gages	27
3.18	Displacement Results of the Propulsion Tank	28
3.19	Strain gage installation process	28

3.20	Quarter-bridge strain gage configuration [14]	29
3.21	Quarter Bridge Amplifier and Internals	29
3.22	Omegadyne PX41S0-30KG5V pressure transducer [15]	30
3.23	Voltage to pressure equation [10]	30
3.24	NI USB-6008 DAQ Card	31
3.25	Test equipment setup diagram	31
3.26	LabVIEW front panel	32
3.27	LabVIEW block diagram	33
4.1	AM propulsion tank with support structure	35
4.2	Four view of the propulsion tank	35
4.3	Flawed features	36
4.4	Flawed and corrected 1cm diameter hole	36
4.5	Von Mises Stress of the Propulsion Tank	37
4.6	Factor of Safety of the Propulsion Tank	37
4.7	Internal pressure during testing	38
4.8	Resulting connector displacement	38
4.9	The rupture seam and close up	38
5.1	SEM pictures of the porous surface	40
5.2	1200x magnification	40
5.3	Unfinished boss and gusset	41
5.4	Visible material porosity around the rupture	41
5.5	Exmaple of lattice structure as internal supports [2]	43

1 Introduction

1.1 Significance of the Study

A number of recent developments have enabled the rapid expansions of pico- and nanosatellites over the past decade. These developments include coordination among pico- and nanosatellites programs, a significant increase in programs, demonstrations showing that pico- and nano-satellites can obtain valuable measurements and improvements in the small satellite technology.

Pico- and nanosatellites offer a number of advantages over the traditional approach of utilizing large government satellites. The most obvious benefit is lower development and launch costs. In addition, many different satellites with different instruments can fulfill the need for more scientific measurements.

Additive manufacturing (AM) is a tool that streamlines and expedites the product development process. In an effort to reduce time to market, improve product quality, and reduce cost, companies of all sizes have come to rely on AM as a mainstream tool for rapid product development [3]. AM significantly impacts the way aerospace companies manufacture products and utilizing additive manufacturing in small satellite application is inevitable [3].

1.2 Purpose Statement

The purpose of this study is to determine if an AM cubesat propulsion tank is a viable material option that will meet and/or exceed the test verification guideline set-forth by the Air Force, NASA, and Department of Defense.

1.3 UNP Constraints

There are a few constraints when designing a propellant tank for cubesat applications, being mass and volume. Due to the nature of the cubesat size, the propellant tank has to be large enough to provide the thrust required by the mission and compact enough to allow for wire management between the subsystem components.

The most important constraint is that the propulsion subsystem has to meet all of the US Air Force's, NASA's and Department of Defenses' standards. These standards and requirements vary from structural testing, material testing, out-gassing, and fracture control.

1.4 Limitations and Assumptions

The largest limitations presented for this research are time, money, lack of usable facilities, and as well as the rapid growth in of AM technologies. Due to the quick turnaround that the University Nanosatellite Program (UNP) required the team to have, the design of the propulsion tank took the majority of the team's effort to finalize. In addition, the time that the structures lab was available for testing was limited in the beginning of the school year, due to the remodeling, which pushed the hardware testing time line back the beginning of the fall semester. In order to fully get the propellant tank spaceflight ready, more testing needs to be conducted, in particular thermal bake-out and vibration testing.

One of the largest limitation is the lack of funding that was provided by this institution. Most of the funding was provided by the Air Force UNP grants. The crucial components were bought first, like the two propellant tanks, but towards the end of the research the lack of available funds slowed down the testing timeline and resulted in a low amount of data collected. Finally, because cubesat and additive manufacturing technologies are new growing industries, it is very difficult to find relevant information that is open to the public and not proprietary information.

2 Review of the Relevant Literature

The propose of this literature review is to define what cubesats are, their current propulsion methods and what the ARAPAIMA cubesat and propulsion subsystem is being designed and built. Additionally, this review also goes over the new industry of AM and the processes available and used in the aerospace industry.

2.1 CubeSat Overview

Cubesats were invented over a decade ago by researchers at California Polytechnic State University, Pomona (CalPoly) and Stanford University to create a standard of university spacecraft [22]. Cubsats fall into the class of research spacecraft in the pico-/nanosatellite category; between 1 and 10kgs. The main reason for miniaturizing satellites is to lower the cost of development and increase the suitability of launching from different platforms by using the excess capacity of larger launch vehicles [20]. With their relatively small size a 1U cubesat, of 10x10x10cm and 1kg, can be constructed with approximately \$10,000 with an additional required \$40,000 to launch it into low earth orbit (LEO) [5].

Cubesats are built to a standard dimension, Units or "U", a 10cm cube with a mass up to 1.33kg and typically uses commercial of the shelf (COTS) components for electronics. Cubesats the scalable along only one axis by 1U (10 x 10 x 10cm) increments. 2U (20 x 10 x 10 cm) and 3U (30 x 10 x10 cm) cubesats have been built and launched since June 2003. A variety of cubesats can be seen in Figure 2.1.

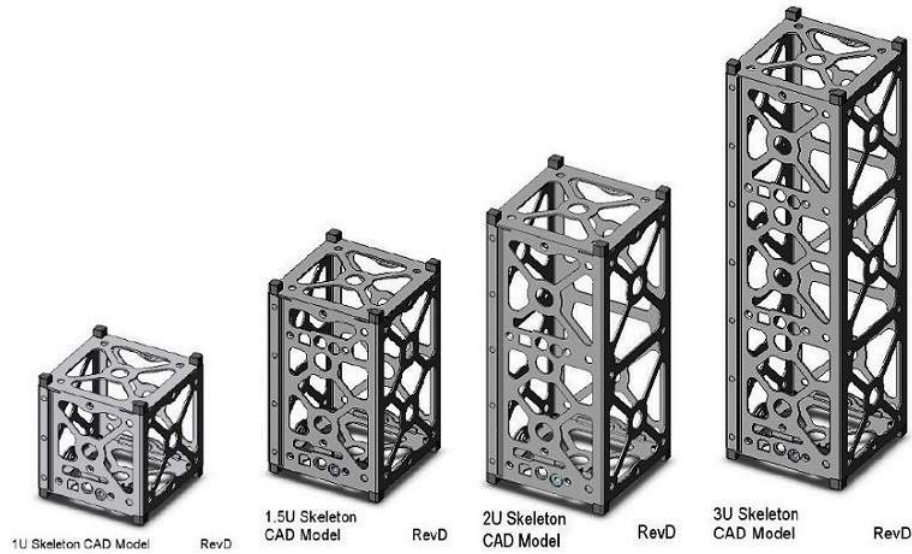


Figure 2.1: Different configurations of cubesats ranging from 1U to 3U [12]

In recent years, larger cubesat platforms have been proposed, most commonly the 6U (30 x 20 x 10 cm) and the 12U (30 x 20 x 20 cm) to extend the capabilities of cubesats beyond academic and technology validation applications and into more complex science and national defense goals. Larger variations of cubesats can be seen in Figure 2.2.

Due to the modularity of cubesats, they can be launched and deployed using a common deployment system. Popular deployment systems that are being used are the Poly-Picosatellite Orbital Deployer (P-POD), Canisterized Satellite Deployer (CSD), NanoRack, built by CalPoly, Planetary Systems Corporation and NanoRacks. The CSD and P-POD can be seen in Figure 2.3. Due to the gaining popularity of cubesats, more companies are building sophisticated and larger capacity deployers. For example, a 3U P-POD has the volume capacity of 3U's, so it can deploy one, two, or three cubesats at once. To date, NanoRacks successfully deployment of 33 cubeSats from the International Space Station (ISS) which was the largest cubesat deployment in history [12].

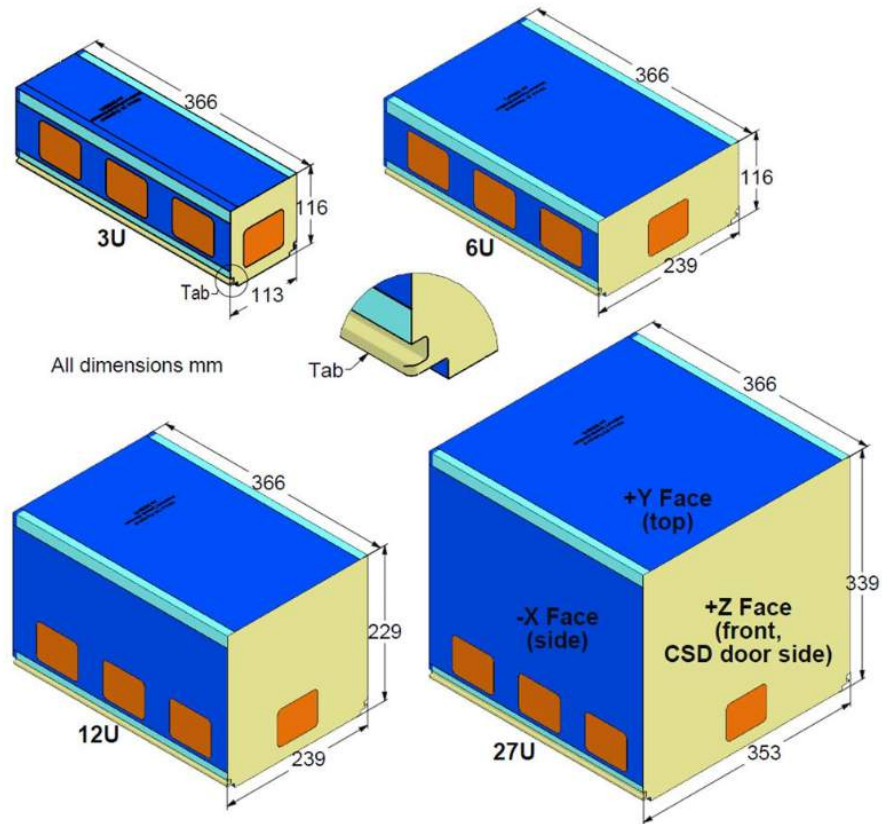


Figure 2.2: Newer and larger proposed cubesat sizes [4]

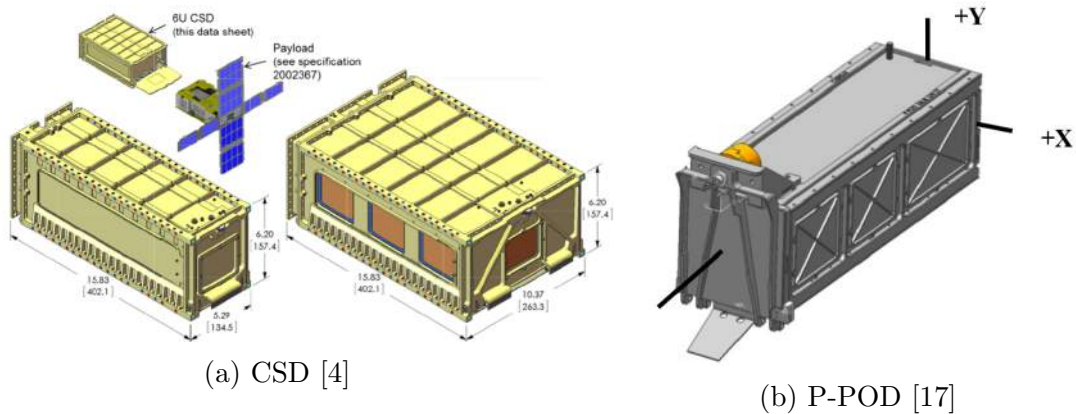


Figure 2.3: Popular cubesat deployers

2.1.1 CubeSat Propulsion

Due to the mass and volume restrictions associated with cubesats, this often necessitates the scaling down of existing technologies or the development of new

technologies that fulfill the duties of the various subsystems [19]. One such subsystem is propulsion. Although propulsion has not always played an important role in the development of small satellite programs, the reason for this has much to do with the inherent complexity involved with propulsion subsystems [21].

The growing interest in the use of nano-spacecraft within the government and industry is driving a critical need for a new propulsion system capable of fulfilling a wide range of mission requirements. These may be needed for fine attitude control, and orbit change maneuvers [20]. The smallest rocket engine technology available today is a cold gas thruster system.

Cold gas thrusters offer an inexpensive, reliable, low-power, nontoxic auxiliary propulsion system for small satellites. They have been used extensively in various attitude control systems providing multiple low-thrust pulses for actions such as attitude control, station keeping, orbit adjustments, docking maneuvers, and trajectory control [6]. The term "cold-gas" means that there is no combustion involved [16]. The actual temperature of the gas can vary. A basic schematic of a cold gas system is shown in Figure 2.4.

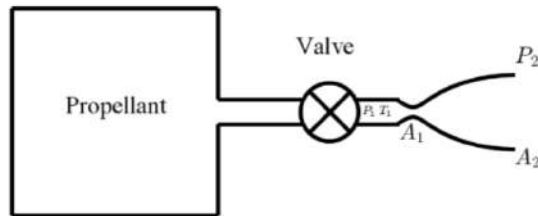


Figure 2.4: Cold-Gas propulsion system schematic [23]

The pressurized propellant is held in a storage tank and released to the expansion nozzle by a valve. Although the simplicity of a cold-gas system seems obvious, the actual thruster system might feature additional components such as a pressure regulator assemblies, filters, and relief valves [23].

2.2 ARAPAIMA CubeSat

Application for RSO Automated Proximity Analysis and IMAGING (ARAPAIMA) is a 6U cubesat that aims to conduct 3D visual and infrared (IR) imaging to resident space objects (RSOs) of interest and its purpose is to demonstrate the power of cubesat technology fields of space situational awareness, reduction of orbital debris and asteroid characterization. An overall view of the ARAPAIMA cubesat can be seen in Figure 2.5 below.

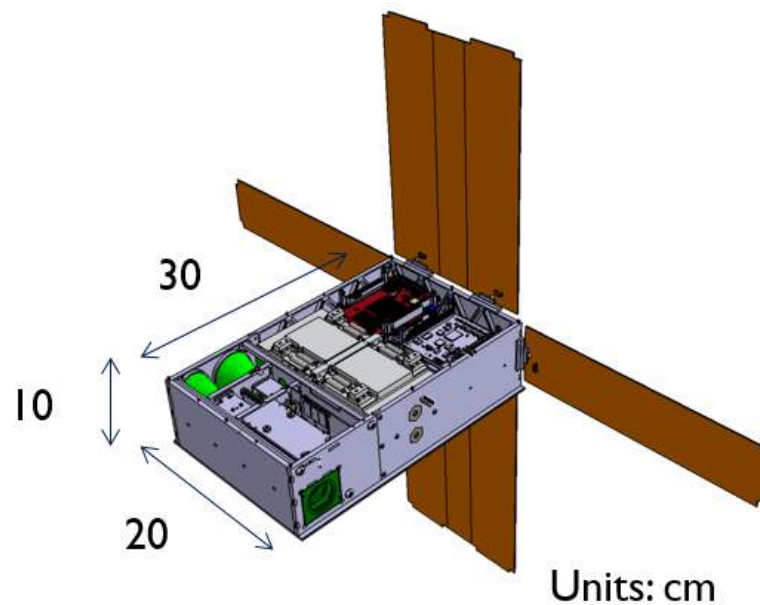


Figure 2.5: CAD model of the ARAPAIMA cubesat

Most of the components on the satellite consists of commercial of the shelf (COTS) components. The payload consists of a commercially available IR camera, monochrome camera and a miniature laser rangefinder with a range of a few km. The payload cameras are installed on the nanosat in the same direction. The cubesat has a star tracker, GPS and an inertial measuring unit (IMU) used for attitude determination and control system. The star tracker is installed in the opposite direction of the payload cameras. The cubesat is equipped with a cold compressed

gas propulsion system which enables it to perform orbital maneuvers and reaction control of attitude. The goal of the mission is divided into four steps: 1) launch and calibrate, 2) approach and track the RSO, 3) complete calibration of visual only navigation (V and V), and 4) image the RSO.

The mission is designed to perform automated proximity and rendezvous operations, demonstrated by missions such as XSS-11 (AFRL) and Orbital Express (DARPA), with a budget two orders of magnitude lower. Successful completion of the mission validates a range of technologies that can be used for debris removal from low Earth orbit by demonstrating robust, affordable, and responsive rendezvous of nanosats with uncooperative RSOs or high value assets (HVA).

2.2.1 ARAPAIMA's Propulsion Subsystem

ARAPAIMA's mission requires a 6U cubesat possessed with a rapid maneuvering capability in order to perform its proximity operations with respect to another spacecraft. Thus, a full 6 Degrees-Of-Freedom (DOF) control system is mandatory. Initially, the team explored the generic use of magnet-torquers, momentum reaction wheels, and micro-thrusters. During the system concepts development phase, the ARAPAIMA control actuators included three sets of momentum wheels to provide fine attitude control, a set of 8 reaction control thrusters to provide course and rapid attitude control, and a single 100mN level thruster intended for orbital maneuvering. The team tried to minimize technology development while keeping in mind the cost of the suitable subsystems.

After critical design review the only type of propulsion system that seemed feasible for ARAPAIMA is the cold-gas thrusters providing both attitude control and orbital maneuvering functionalities; allowing the team to eliminate the 3 momentum reaction wheels that were expensive, \$30,000 a piece and heavy. The unique capability of the cold gas thruster system is due to its thrust level overlapping the needs

of both type of maneuvers, ease of integration/modification, and low cost (based on the student built price of \$1000 per thruster) [13]. Propulsion system redundancy is then added by doubling the amount of nozzles from the original 8 to 16 which can be seen in Figures 2.6 and 2.7.

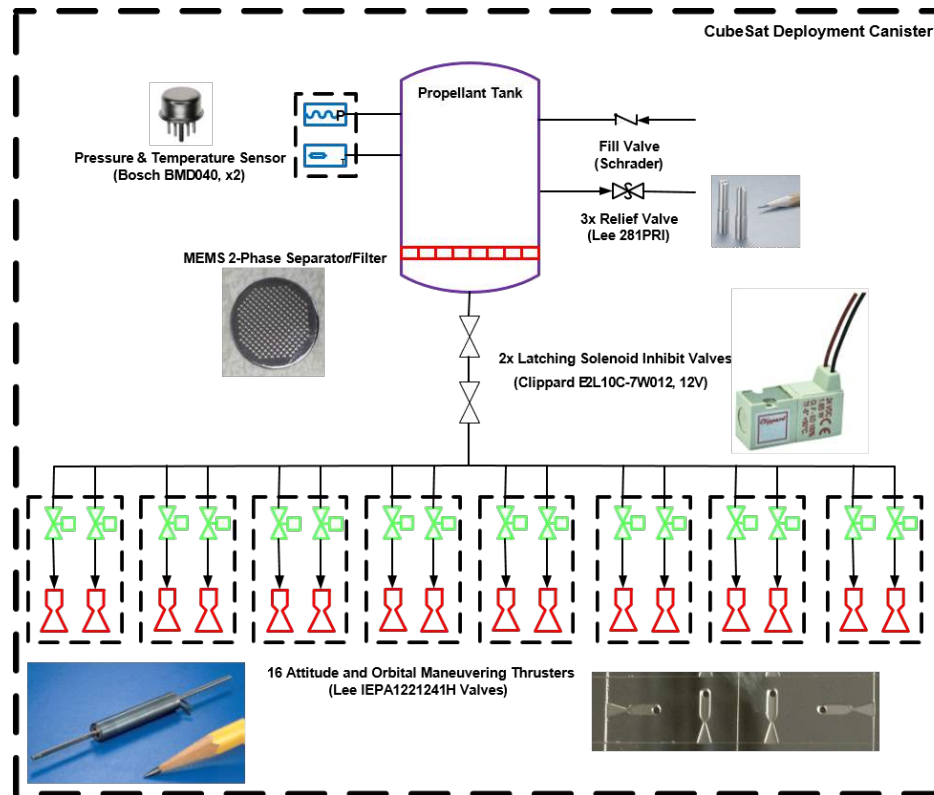


Figure 2.6: ARAPAIMA's Propulsion Fluidic System Diagram

The overall ARAPAIMA propulsion system is shown in Figure 2.6 at the heart of which is the propellant tank holding 2-phase fluids (saturated fluids or also called a liquefied gas under compression). Due to the physical properties of the expected propellant, the propellant tank is considered as a pressure vessel under NASA-STD-5003 Pressure Vessel definition. Alternatively it is defined as Hazardous fluid or fluid container per NASA-STD-5003. Since the efficient operation of the microthrusters require the gaseous phase of the propellant to be separated from the saturated phase inside the tank, micro-fabricated silicon chips with through holes act as the phase separator based on the expansion-valve principles; while the holes act simultane-

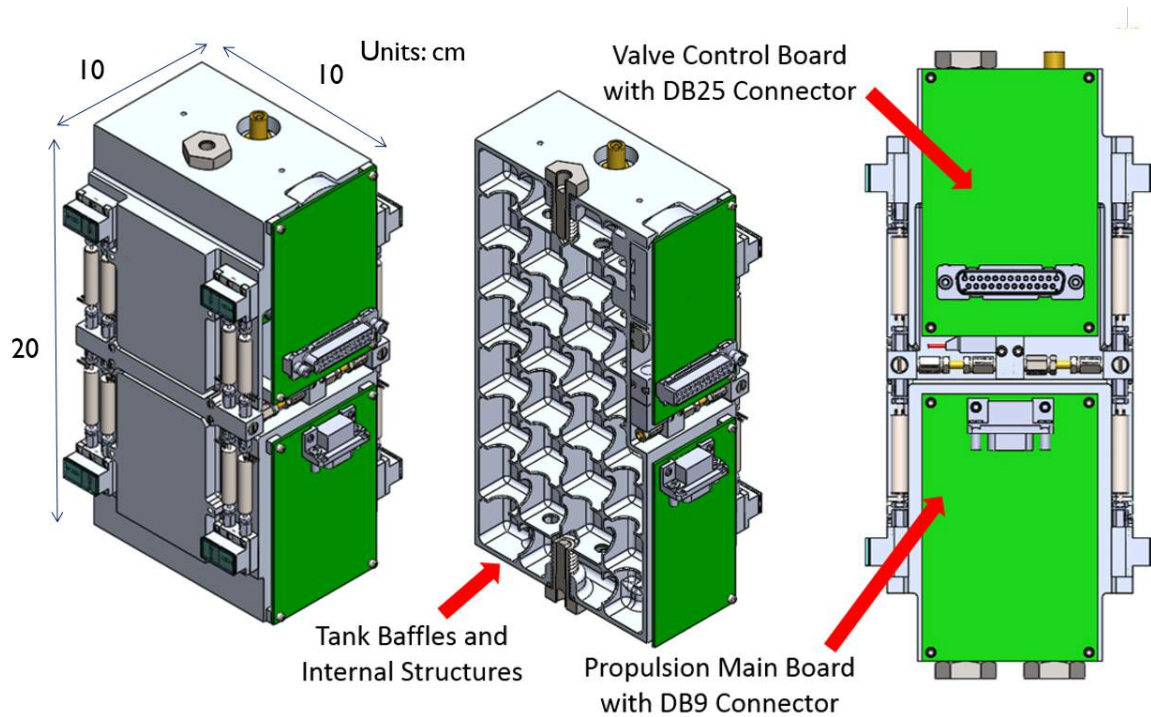


Figure 2.7: ARAPAIMA's Detailed Propulsion System

ously as the coarse filter to prevent inadvertent debris in the fluidic system. After passing through the phase separators, the gaseous propellant is then contained by two latching solenoid inhibit valves. A common manifold then follows the latching valves to feed the individual thruster nozzles via a solenoid valve (16 in total). The nozzles are fabricated from single crystal silicon wafers capped by thermal-stress resistant borofloat glass (similar to Pyrex) using anodic bonding. Also mounted to the propellant tank are two sets of pressure and temperature sensors acting as real-time monitoring transducers and 3 pressure relief valves selected to define the Maximum Design Pressure (MDP) as specified in NSTS 1700.7B [8].

ARAPAIMA's propulsion system will follow the maximum possible of the requirements set-forth in the relevant standards and requirements. It consists of triple redundant pressure relief for the propellant tank. The fluidic system incorporates two latching valves as inhibits, in conjunction with the unpowered state of the spacecraft as the third inhibit, and finally the deployment canister as a fourth in-

hibit acting as a physical containment in the event of catastrophic release of high pressure fluids.

2.3 Additive Manufacturing Overview

Additive Manufacturing (AM) refers to a process by which digital 3D design data is used to build a component in layers by depositing material. AM can be alternatively called direct digital manufacturing, free form fabrication, or 3D printing. The term "3D printing" is increasingly used as a synonym for AM as explained before. However, the AM is more accurate in that it describes a professional production technique which is clearly distinguishable from conventional methods of material removal, also known as subtractive manufacturing.

Since the first technique for AM became available in the late 1980's, it was primarily used to fabricate models and prototypes. AM technology has matured and experienced more than 20 years of development and is presently one of the rapidly developing advanced manufacturing techniques in the world. Today AM is on the step to serial production in industries ranging from aerospace and medical to energy and automotive benefit from the possibility to design and manufacture products in a completely new way [3]. The components produced by AM technologies are no longer merely used for visualization but are also used as real production parts with basic mechanical properties meeting and sometimes exceeding the industry standards and requirements.

AM systems may be classified/categorized in terms of the material feed stock, energy source, and build volume. Another approach is to collect processes together according to the type of raw material input, but this thesis we will be focusing on powder bed fusion processes [9].

2.3.1 Powder Bed Fusion Processes

Powder bed fusion is a process that utilizes thermal energy fuses selective regions of a powder bed. The source of the thermal energy is a laser or an electron beam. The thermal energy melts the powder material, which then changes to a solid phase as it cools. A schematic of the PBF process can be seen in Figure 2.8. Terms that are also used in the AM industry for powder bed fusion processes and systems include laser sintering, selective laser sintering, selective laser melting, direct metal laser sintering, and electron beam melting.

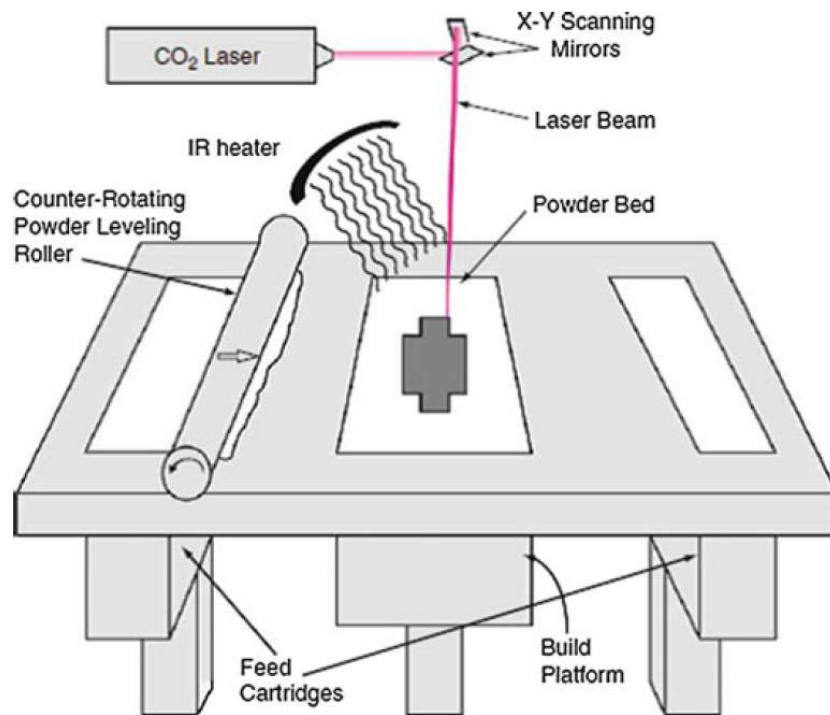


Figure 2.8: Generic schematic of an AM powder bed fusion system [9]

Both polymer and metal materials are available in powder bed fusion processes. For polymers, the unfused powder surrounding a part serves as a fixturing system, so no additional supports are usually needed [9]. For metal parts, anchors are typically required to attach part(s) to a base plate and support down-facing surfaces. This is necessary because of the higher melting point of metal powders. Thermal gradients

in the build chamber are high, which can lead to thermal stresses and warping if anchors are not used [7]. Because powder bed fusion is a thermal process, warping, stresses, and heat-induced distortion are potential problems for all materials [3].

Laser-based powder bed fusion systems generally produce a better surface finish and finer feature detail than electron beam systems. Electron beam systems are somewhat more expensive, but are faster. Also, electron beam systems produce less residual stress in parts, resulting in less distortion and less need for anchors and support structures [7]. Powder bed fusion systems are relatively expensive compared with most other AM processes, especially the machines that process metals. Operating costs are comparatively high due to the cost of materials, the recycling issues with polymer powders, and the facility requirements for inert gas and safety. Parts made on these machines are being used increasingly for final products, so manufacturers have begun to include process control capabilities in the machines to ensure process quality and repeatability [7].

2.4 Hypothesis

The aerospace industry has used AM technology since it was introduced because AM gives the ability to generate complex geometries with limited number of manufacturing steps. This new technology is a feasible option to use in the cubesat community due to its low cost to build final flight ready components. The materials available should meet and exceed industry standard and provide a viable propellant tank for the ARAPAIMA cubesat.

3 Methodology

This sections explains and shows the design process of the propellant tank both pre- and post- manufacturing, why and how modifications where made for both the AM process and hardware testing, and the equipment used for the hardware testing.

3.1 Research Approach

The goal is to test the hypothesis, therefore the most basic requirement that was followed is:

”UNP 2. The smallsat shall be designed to withstand the launch and on-orbit environments of the launch vehicle without failure, leaking fluids, or releasing anything.” [1]

3.1.1 Tank Design

When designing the ARAPAIMA mission there was a minimum amount of delta V or thrust that was required to complete the mission. From that the propulsion subsystem had requirements such as size, material, and mass constraints that will be explained in further detail in the next sections.

3.1.1.1 Size Constraints

The propulsion subsystem team was given a 2U or 10x10x20cm space in the center of the cubesat as seen in Figure 3.1. Therefore the propulsion subsystem

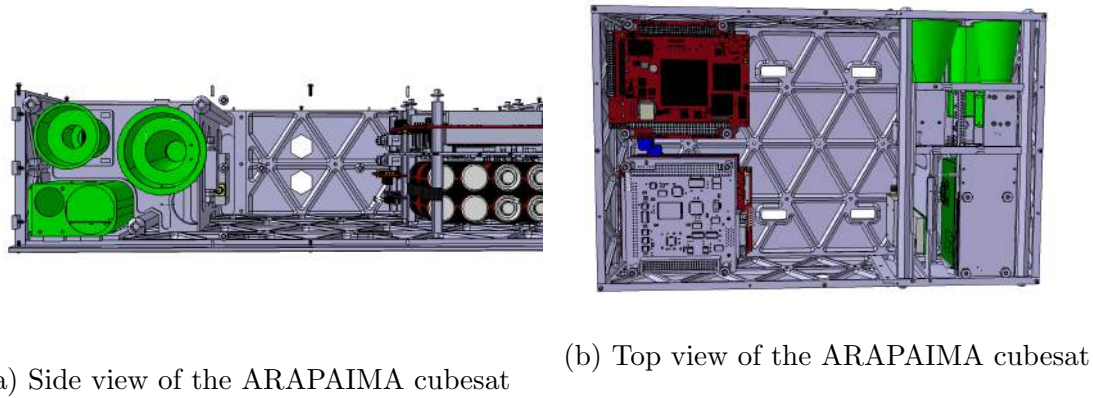


Figure 3.1: 2U of space available for propulsion subsystem

team started designing the tank by simply making a visual model out of foam as seen in the design progression Figure 3.2. These physical models were a great visual aid and played an important role in making sure everything fit together as seen in Figure 3.3.

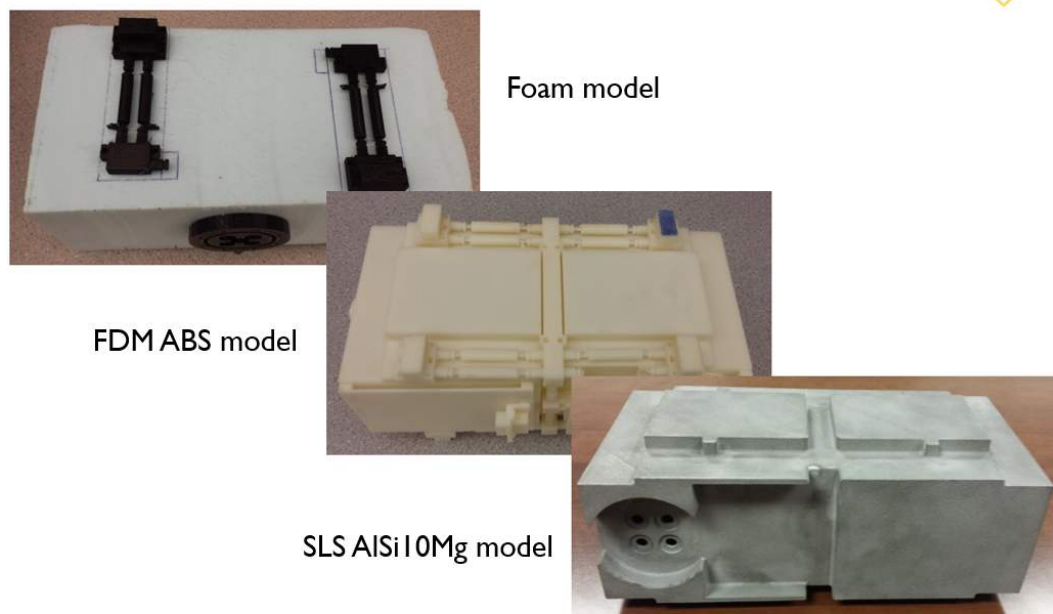
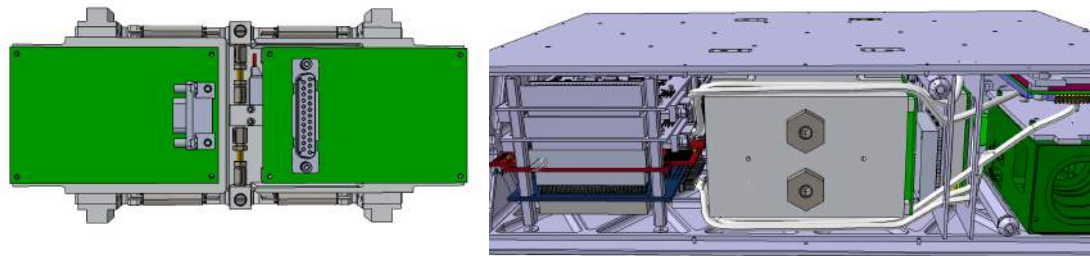


Figure 3.2: Design iterations of the propulsion subsystem

As the remaining subsystems got more complicated, the propulsion subsystem had to shave of some size and allow channeling for wire management since the



Figure 3.3: ARAPAIMA cubesat fit check



(a) Front view of propulsion tank with wire management channels

(b) Side view with wiring in place

Figure 3.4: 2U of space available for propulsion subsystem

payload was on one side of the cubesat and the the power and computer stack were in the other. The channeling was made on each corner of the propulsion tank which can be seen in Figure 3.4.

3.1.1.2 Material Constraints

When selecting the materials of the propellant tank we had some basic requirements that were given to us by the UNP User's Guide, ARAPAIMA's systems engineers team and what the company manufacturing the propellant tank had available.

Due to ARAPAIMA's budget, manufacturing the propellant of tank of a polymer was the first thought because it was a cheaper alternative to composites and metals.

The AM of plastic products can make use of polyamides (PA), polystyrenes (PS), thermoplastic elastomers (TPE), and polyaryletherketones (PAEK), all of which are readily available by our manufacturer. Unfortunately, these materials do not meet the out-gassing requirements that UNP requirement number nine set forth which is listed below.

”UNP 9. Use of non-metallic material shall be restricted to materials that have a maximum collectable volatile condensable material (CVCM) content of 0.1% or less and a total mass loss (TML) of 1.0% or less.” [1]

Another option was was manufacture the propellant tank out of a composite material like NASA, JPL, and other DoD contractors build. Due to the nature of the UNP program and all of the participants being universities, the UNP Users Guide highly discouraged the use of composite materials as listed below.

”Use of composite primary structures including traditional non-metallic composite structures, metallic structures built up using adhesives, and bending as a means of forming metallic primary structures, is highly discouraged!” [1]

Therefore a metal AM propellant tank was our only choice. The EOSINST M280 sintering machine is the machine used by the manufacturer and offers a wide range of metal powders that can be used for our purpose such as aluminum AlSi10MG, Colbalt Chrome MP1 and Sp2, Maraging Steel MS1, Nickel Alloy HX, IN625, and IN718, Stainless Steel GP1, PH1, and 316L and Titanium Ti64-Ti6Al4V and Ti64EL1. The wide variety of materials offered a very high degree of flexibility in design and development.

A requirement that was set by ARAPAIMA’s systems engineering team was to minimize the weight of the propellant tank due to the strict 12kg overall weight of our 6U cubesat. This eliminated the Colbalt Chrome, Maraging Steel, Nickel Alloy, and the Stainless steel options, which left us with either the aluminum or titanium alloy as a suitable material option.

In order to minimize casualties resulting from reentry debris, it is recommended that materials with high melting points (e.g. steels, titanium alloys) not be used as structural materials as listed in UNP requirements number 14 as seen below.

”UNP 10. All materials with a melting point high enough to allow a sample to reach the earth with greater than 15 joules of energy are prohibited.” [1]

Which leaves us with using AlSi10MG, the strength properties of which is similar but slightly superior to the 6061-T6 aluminum alloy, whose material datasheet can be seen in Appendix B. The manufacturer’s datasheet also provided a single fatigue strength test case of 977 MPa load at 50Hz, stopped at 5 million cycles without fracture, which is similar to that expected from wrought aluminum alloy.

3.2 Propellant Tank Modifications

After meeting the size and material constraints the propellant tank is then slightly modified for the AM process and hardware testing as explained in the sections below.

3.2.1 Design Modifications for AM

AM presents both opportunities and challenges. On the positive side, it offers greater design freedom through the ability to produce shapes that would be otherwise impossible or prohibitively expensive [3]. Examples include highly organic external forms, intricate internal structures as you will see Figures 3.5 and 3.8. This geometric freedom can be exploited to create products with more appealing aesthetics, improved ergonomics, and enhanced functional performance. For example, a set of design rules for selective laser melting was sent to us after sending the initial CAD model to the propellant tank manufacturer. They recommended some design tips and changes that will ease the manufacturing process and make the part producible

as seen in Figure 3.5. After reviewing their suggestions, the propellant tank was then orientated at 45 degrees, smaller holes were removed and added gussets to the bosses as explain in these further sections.



Figure 3.5: Recommend design modifications for the AM process

3.2.1.1 Build Orientation

The orientation of a part with respect to the primary build axis significantly affect support generation and removal [9]. The build process includes a method called self-supporting angle. This is the angle in which the model material can support itself without the use of support material. If you can build this into your model you will save a ton of time and money. The Figure 3.6 below shows a cantilevered parts of the model and how the angle of the part affects the products finish.

PBF techniques for metals require support structures to resist distortion and are built from the build material. The development of the support material is design to

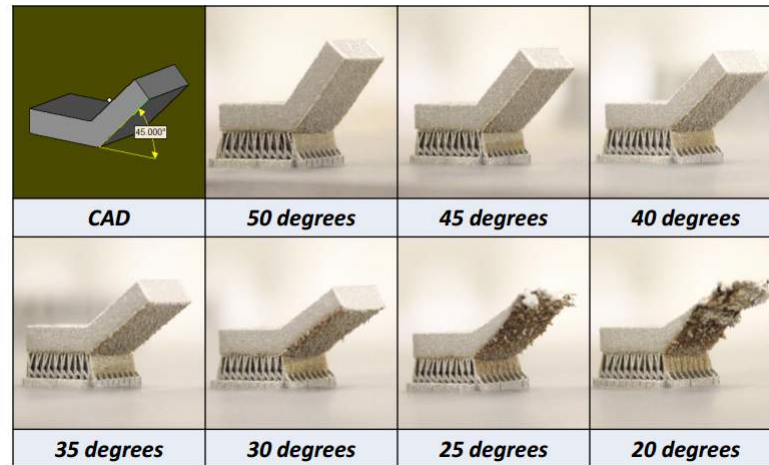


Figure 3.6: Self supporting angles of 316L Stainless steel with 30 micron layers [18]

ease the removal of the material in post processing. The support structure that was used for the propulsion tank is colored in purple in Figure 3.7.

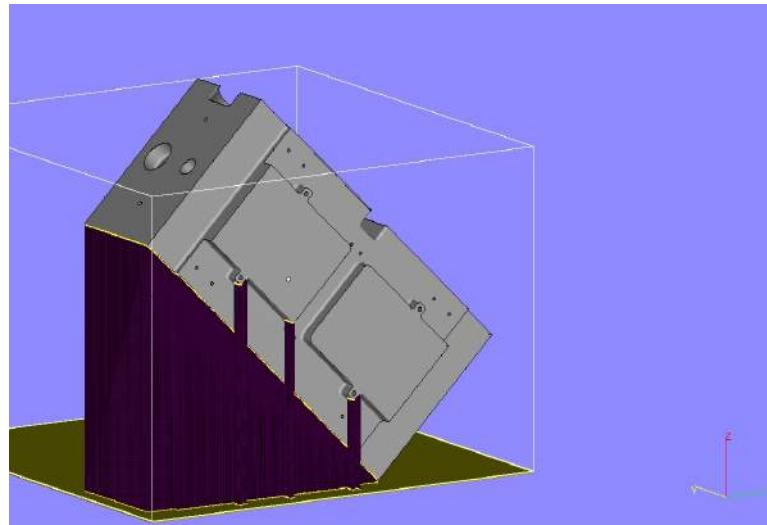


Figure 3.7: Build Orientation with support structure

3.2.1.2 Bosses, Gussets, and Hole Diameters

Bosses that were added to accommodate the hardware interfaces like the pressure transducer, plugs and valves were increased to ease the manufacturing process. Gussets were also added so that the cantilevered boss which is at a 45 degree angle can have some support material which can be seen in Figure 3.8.

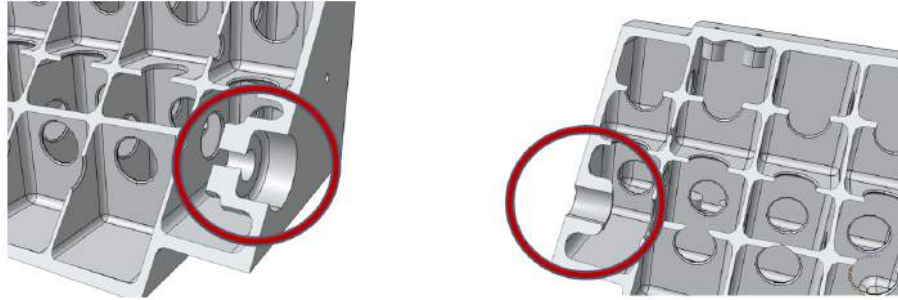


Figure 3.8: Bosses increased to accommodate the AM process

The holes that were in place to use as attachment points for the inhibit valves, electronics, and harnessing in Figure 3.9 were removed in order to precisely drill and tap in a later process.

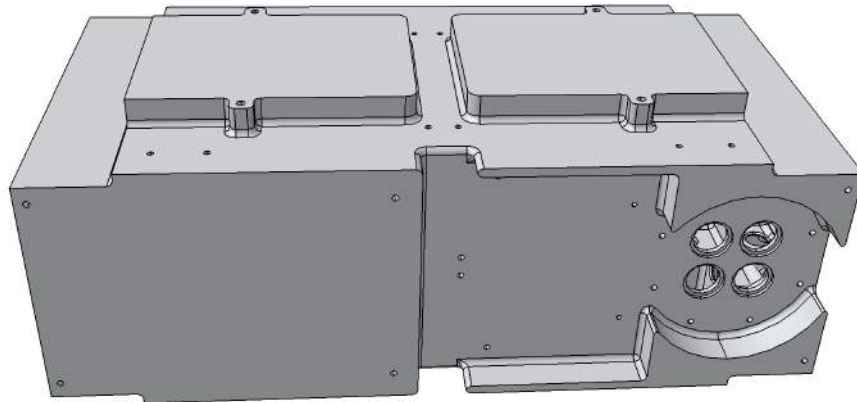


Figure 3.9: Harnessing holes that will be removed to be precisely machined later

3.2.2 Hardware Modifications for Testing

Once receiving the propulsion tank back from the manufacturer it was prepared and post processed for testing. The holes that were left there so that the powder can be removed were drilled and tapped. The left side had two screw plugs and the two on the right were left vacant for the hydrostatic pressure system interfaces as seen in Figure 3.10. The four holes that were in the front face had too small of



(a) Two screw plugs



(b) Hardware interface side

Figure 3.10: Drilled and tapped holes for testing

a wall thickness to have a fine threaded screw plug to fully latch, therefore small metal plugs were machined and enclosed in weld to fully withstand the pressure of the testing which can be seen in Figure 3.11.



(a) Four holes to be welded shut



(b) Results of the welding process

Figure 3.11: Before and after of the front four holes

3.3 FEA Study

A finite element analysis (FEA) study was conducted in order to see if the propellant tank would be able to withstand at least the minimum 1.5 x maximum design pressure (MDP). The operating pressure of the propulsion subsystem would be 120 psia, therefore the minimum proof pressure would be 160 psia. The FEA study was

done in Solidworks Simulation workbench, but before starting the study, smaller features of the propulsion tank were removed in order to reduce the calculation time of the analysis but mainly due to the computer not being able to mesh small features without crashing. The features that were mainly removed were the small fillets, in the outside edges as well as in the internal baffles, which can be seen in Figure 3.12.

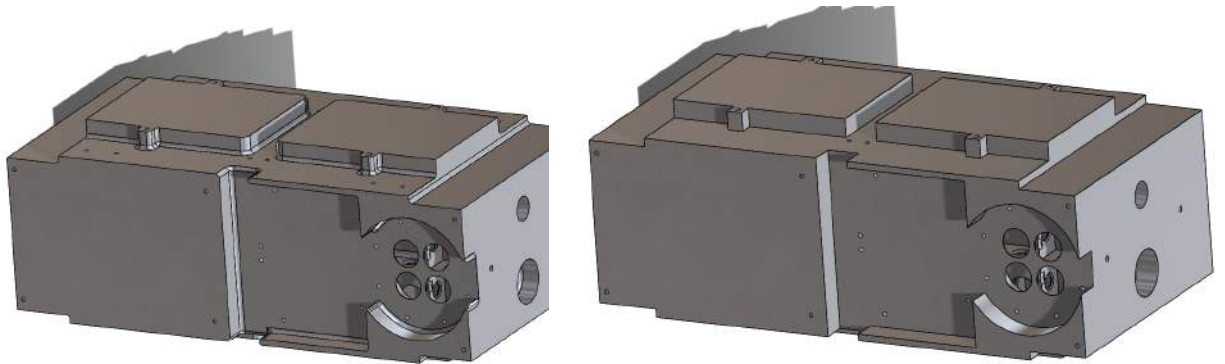


Figure 3.12: Propellant tank features removed for mesh generation

The propulsion tank was fixed where the testing hardware interfaces will be connected as well as the plugs, as seen in Figure 3.13. Then an outward pressure of 160 psia was applied to the propulsion tank which is seen in Figure 3.14. The results of the FEA will be presented in results section, together with the experimental results.

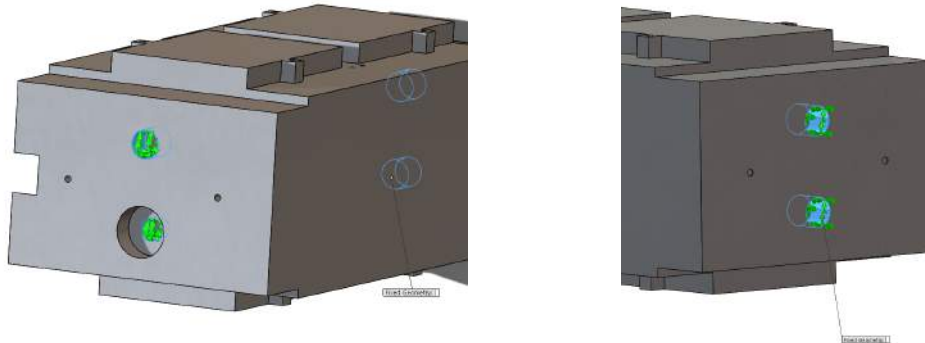


Figure 3.13: Fixed support applied to the hardware interface holes

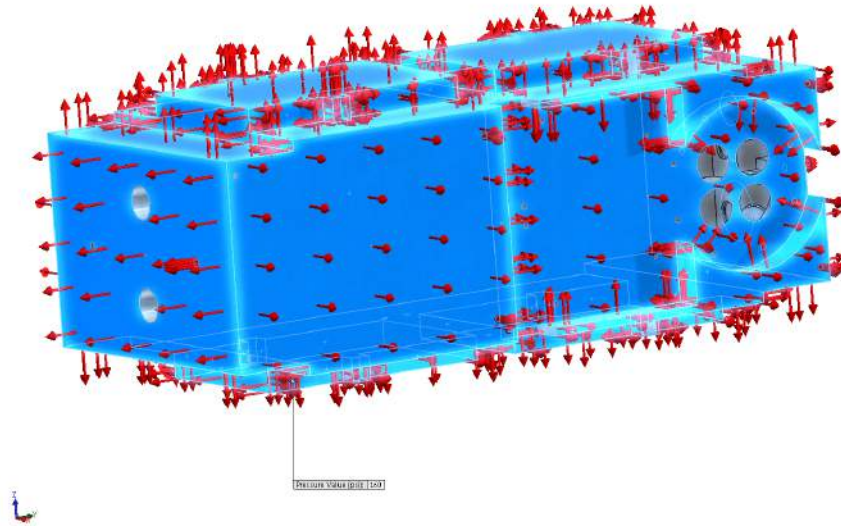


Figure 3.14: 160 psi of outward pressure applied to the surface

3.4 Experiment Testing Equipment

The following sections explain the equipment that was used to test the propulsion tank.

3.4.1 Hydrostatic Pressure Test System

Standard hydrostatic pressure testing procedures entail filling the test vessel with liquid, bleeding out air and then pressurizing it. The test is performed with an incompressible liquid, usually water, because it will only expand by a very small amount should the test piece fail and not pose a high danger like air. Water is our most commonly used test medium because it is less expensive than oil, an easier method to set up than air.

The hydrostatic pressure chamber that was used is located in the Structures lab in the Lehman building and its basic schematic can be seen in Figure 3.15. The hydrostatic pressure chamber uses a pneumatic driven piston pump with two check valves to prevent back flow. The pump operates on 10-100psi air pressure input which also controls the output. The pump will output up to 18,500psi with 100psi

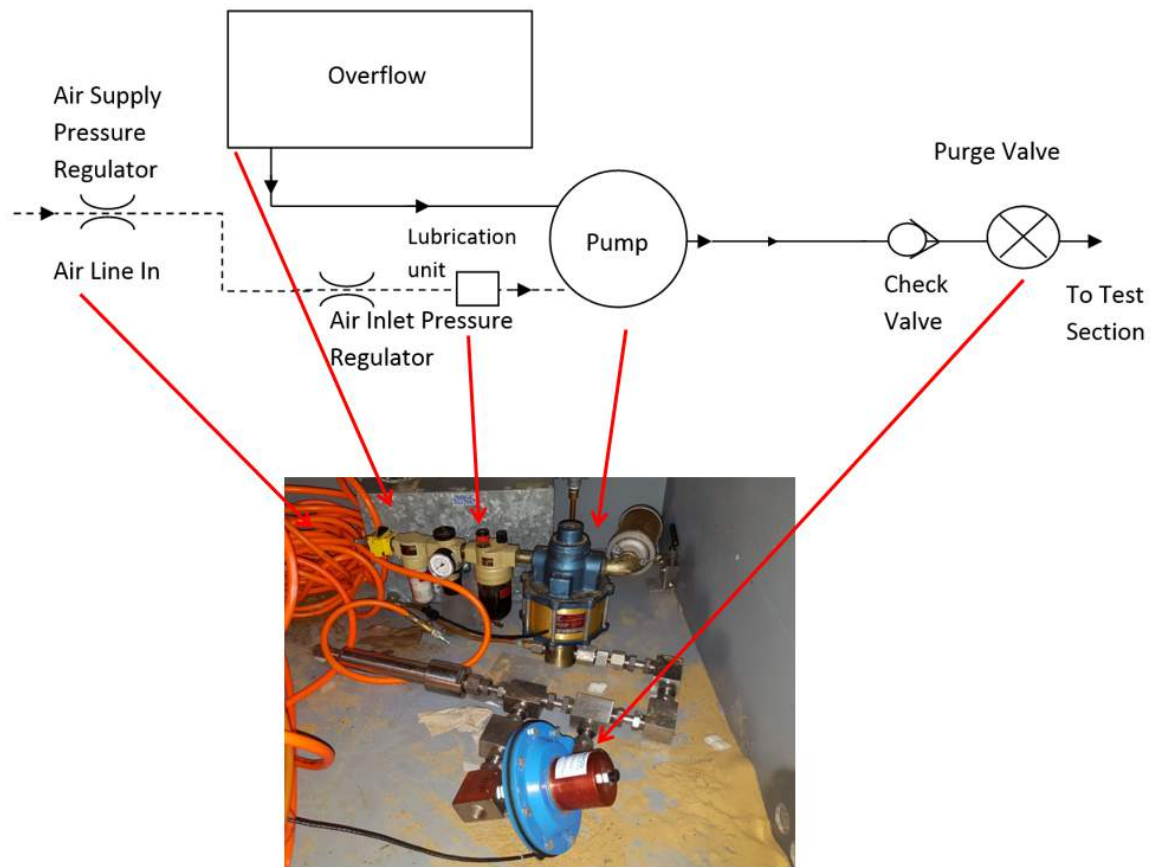


Figure 3.15: Hydrostatic Chamber Schematic and physical system

air pressure input. The testing equipment is fully enclosed in a steel box to not only protect the facilities but the experimenter as seen in Figure 3.15.

3.4.2 Strain Gage

All strain gage configurations are based on the concept of a Wheatstone bridge which can be seen in Figure 3.16. A Wheatstone bridge is a network of four resistive legs. One or more of these legs can be active sensing elements. The Wheatstone bridge is the electrical equivalent of two parallel voltage divider circuits. R_1 and R_2 compose one voltage divider circuit, and R_4 and R_3 compose the second voltage divider circuit. The output of a Wheatstone bridge is measured between the middle

nodes of the two voltage dividers.

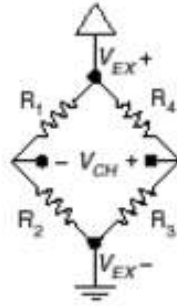


Figure 3.16: Basic Wheatstone Bridge Circuit Diagram [14]

A change in strain applied to a specimen or a temperature shift, changes the resistance of the sensing elements in the Wheatstone bridge and there are three types of strain-gauge configurations: quarter-bridge, half-bridge, and full-bridge.

The strain gages were purchased from OMEGA and the model number were SGD-10/350-LY43 which can be seen in Figure 3.17. The resistance of each strain gage is $350\Omega \pm 0.33$ with a strain gage factor of 2.09. Six strain gages were installed on the surface of the propellant tank that had relatively large deformations while pressurized as seen in the FEA study in Figure 3.18. The strain gages were numbers according to which face they were installed in, 1 and 2 were in the front face, 3 in the bottom face, 4 on the top and, 5 and 6 on the back face as seen in Figure 3.19.

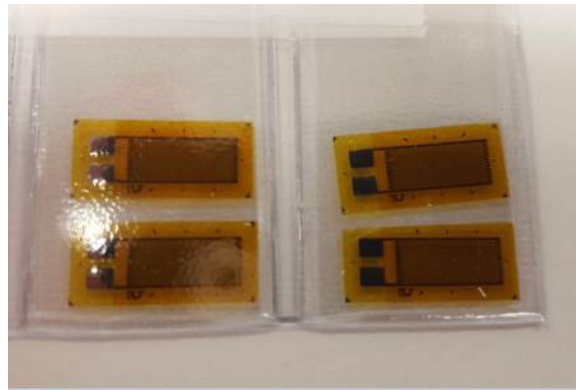


Figure 3.17: Purchased strain gages

The strain gages and bonding terminals were installed using the Vishay Micro-

Measurements Instructions Bulletin B-127-14 [14]. Then 2 wires were then soldered from to the strain gage to the bonding terminal and then each wire was labeled with respect to its channel.

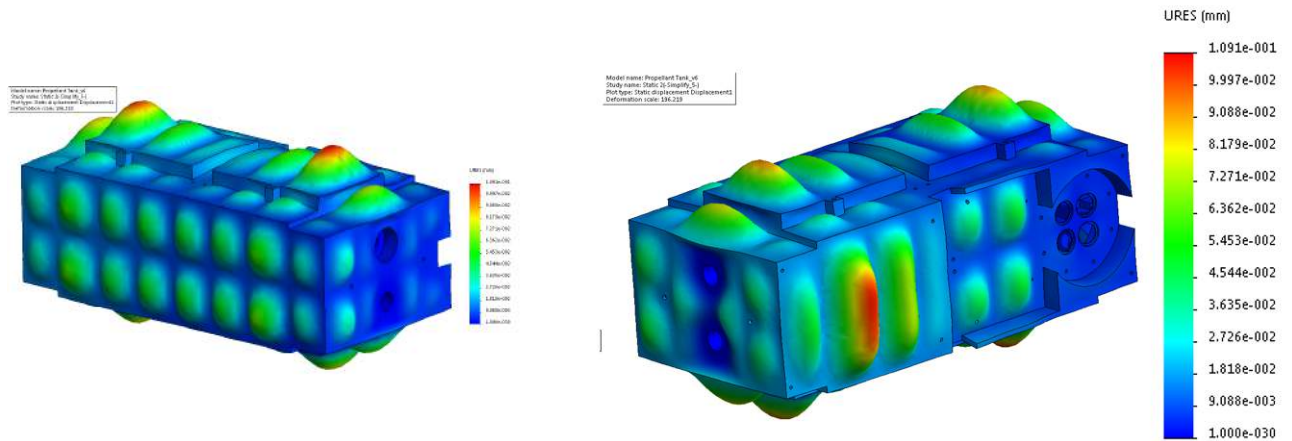
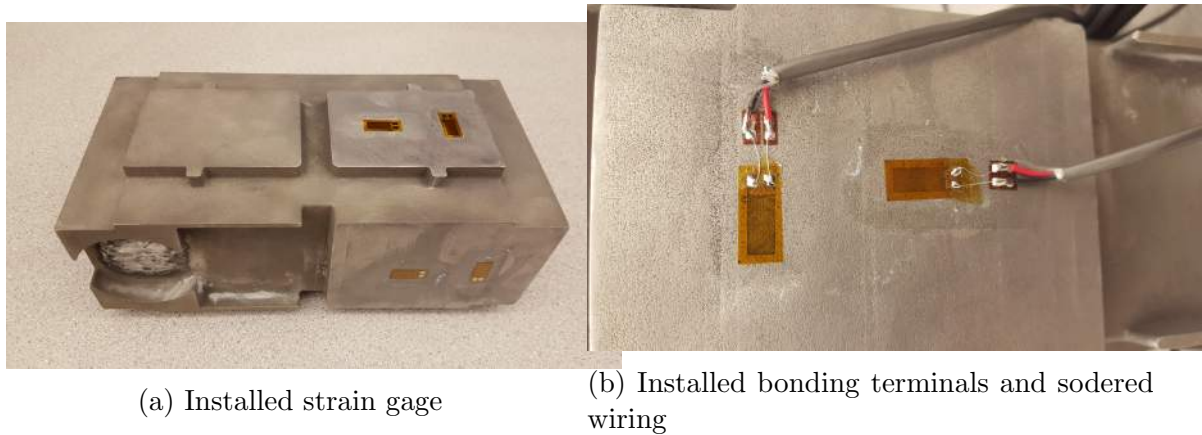


Figure 3.18: Displacement Results of the Propulsion Tank



(a) Installed strain gage

(b) Installed bonding terminals and soldered wiring

Figure 3.19: Strain gage installation process

Mike Potash, an ERAU Electronics Technician, had previously created quarter bridge and amplifier for each one of the strain gage channels. A quarter bridge consist of three 350Ω resistors along with the 350Ω strain gage seen in Figure 3.20. An excitation voltage(V_{ex}) of 8.19 VDC is applied to the quarter bridge for each channel and the lead resistance (R_L) is measured to be 0.04Ω .

The output of each one of the quarter bridges is applied to a 1000 gain ampli-

fier. A potentiometer on each channel allows the balancing of each channel before testing because an unstrained strain gage should have zero voltage. Balancing was performed, for each channel, right before testing the tank and after all wires and equipment where in their final positions. These balancing potentiometers can be seen in Figure 3.21 as well as some of the internal components of the quarter bridges and amplifiers.

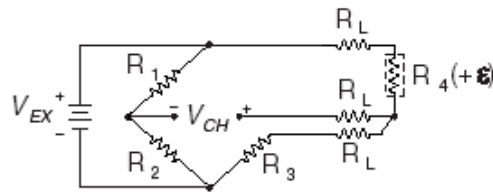


Figure 3.20: Quarter-bridge strain gage configuration [14]

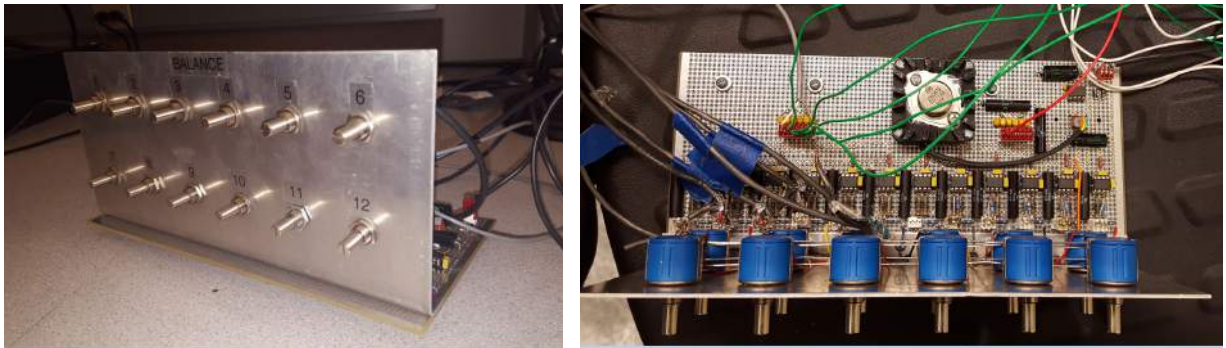


Figure 3.21: Quarter Bridge Amplifier and Internals

3.4.3 Pressure Transducer

An Omegadyne PX41S0-30KG5V pressure transducer was used to measure the internal pressure during the test and is shown in Figure 3.22. The pressure transducer requires an excitation voltage range of 10 to 40 VDC, has an output range of 0.5 to 5.5 VDC and can measure pressure from 0 to 30,000 psi; all of which are within the range of this test. During the testing, a Mastech DC power supply HY3005F-3 provided 32V of excitation to the pressure transducer.



Figure 3.22: Omegadyne PX41S0-30KG5V pressure transducer [15]

The pressure transducer outputs a voltage signal and must be converted to units of pressure using the equation in Figure 3.23 [10].

$$\text{Pressure} = \left(\frac{C_{fs}}{V_{ex}} \right) \left(\frac{V_{meas}}{CF} \right), \text{ where}$$

C_{fs} = Full Scale Capacity - the maximum pressure which the transducer should receive

V_{ex} = Excitation Voltage - the recommended input voltage

V_{meas} = Measured Voltage - the raw voltage returned by the sensor

CF = Calibration Factor - the output of the transducer, usually expressed in mV per input V

Figure 3.23: Voltage to pressure equation [10]

3.4.4 Data Acquisition Cards

Two NI USB-6008 data acquisition (DAQ) cards, which can be seen in Figure 3.24, were used during the hydrostatic pressure test to accommodate the six strain gage channels and one pressure channel. One card was connected with strain gage channels 1-4 and the other one with strain gage channels 5-6 as well as the pressure transducer channel.

3.4.5 LabVIEW

LabVIEW is a highly productive development environment for creating custom applications that interact with real-world data or signals in fields such as science



Figure 3.24: NI USB-6008 DAQ Card

and engineering [11]. For the testing LabVIEW 2012 was used to acquire all the data from the DAQ cards. A test equipment set up diagram seen be seen in Figure 3.25 which shows how everything is connected and powered up, from the strain gages to LabVIEW code.

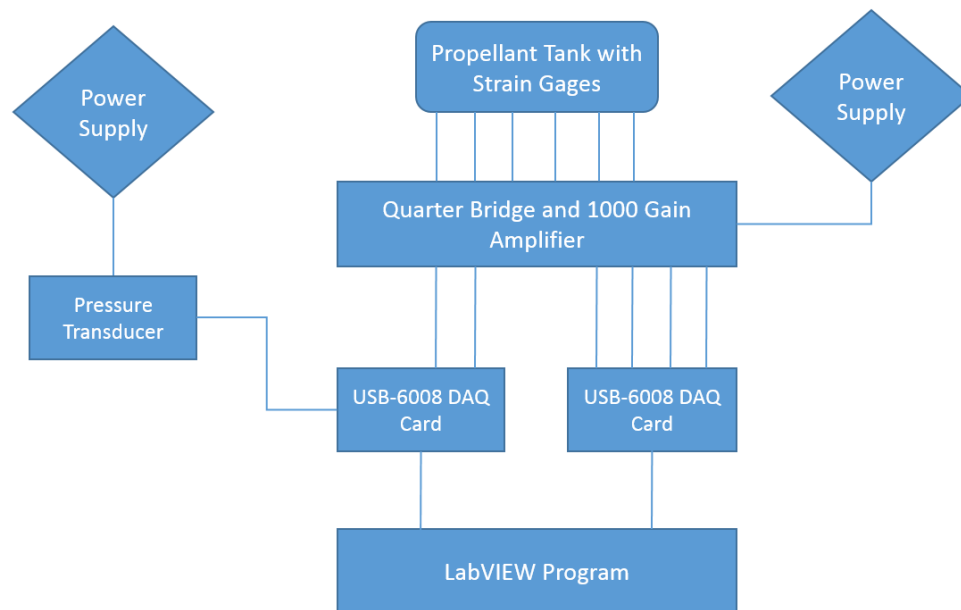


Figure 3.25: Test equipment setup diagram

A LabVIEW program was created to view the all six strain gage data and pressure transducer data which came as a voltage readout which would be calculated

into pressure later. The Figure 3.26 you can see a graphic user interface (GUI) which shows all seven channels. A VI program was also created to assign which graph represented which channel and also programmed to save all the data to be analyzed at a later time.

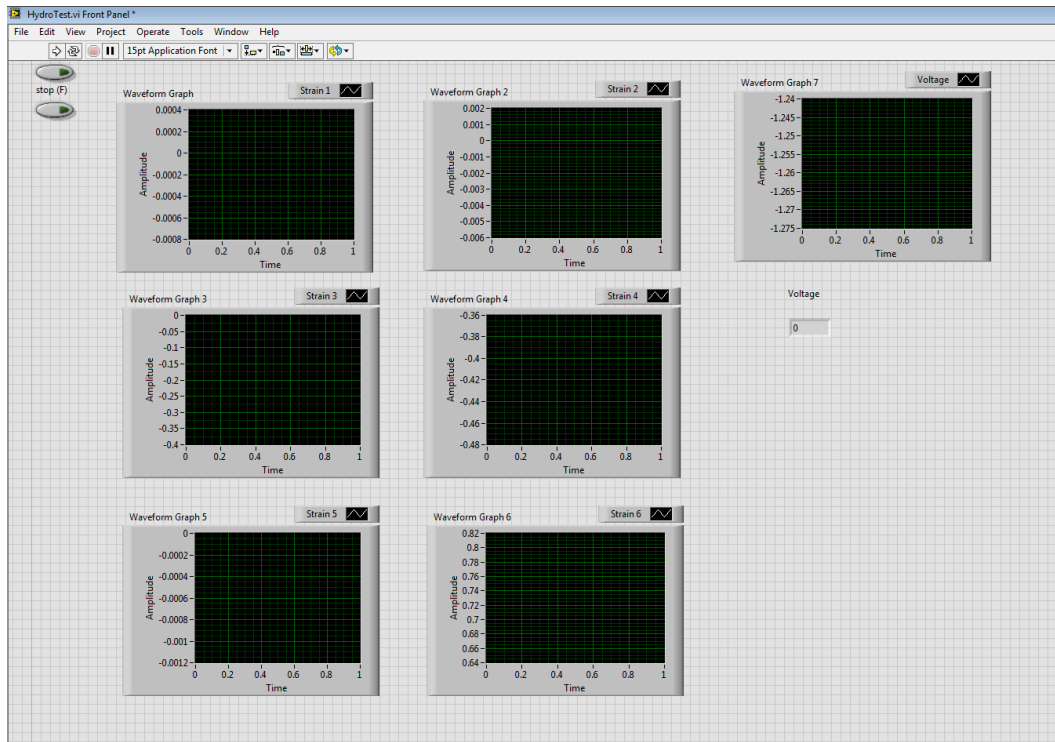


Figure 3.26: LabVIEW front panel

Figure 3.27 shows how the GUI in LabVIEW was created. The DAQ assistant tool was used to acquire the signals from the strain gages and then a different block was used to select which channel you wanted. Afterwards you select which time out output you want and for this, the graphical block as used. The square in the left shows strain data channels 1 to 4 and the right square shows strain data channels 5 to 6 as well as the pressure transducer channel.

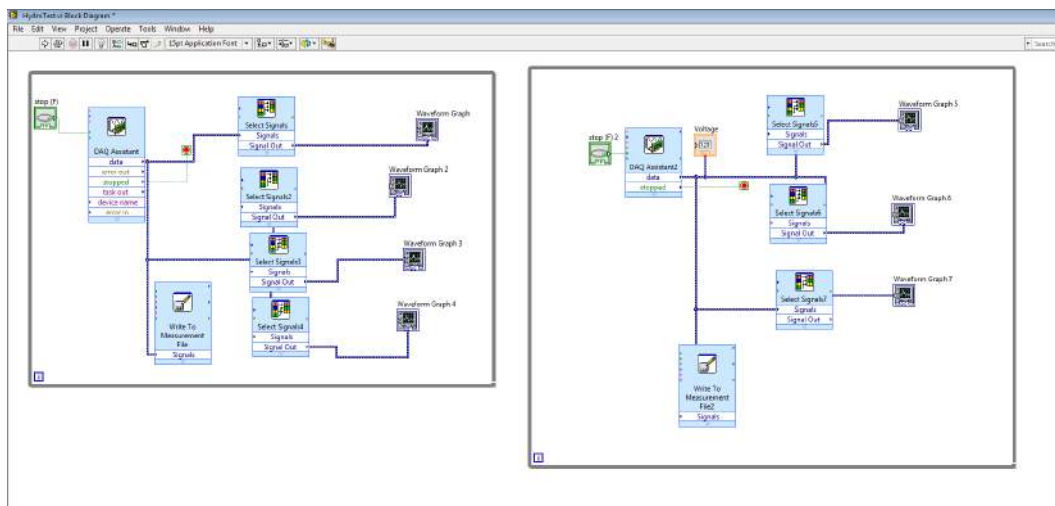


Figure 3.27: LabVIEW block diagram

4 Results

4.1 Additive Manufacturing Results

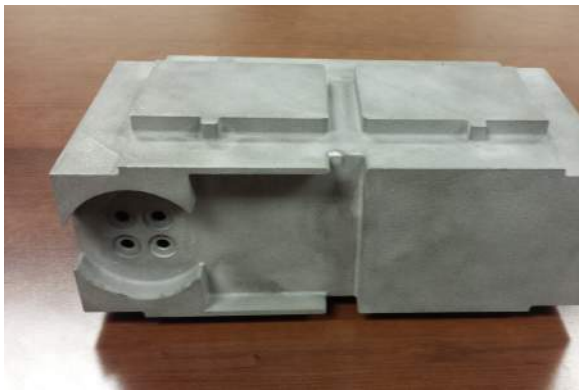
Two propulsion tanks were manufactured, one for non destructive testing and the other for destructive testing. The total print time to make the tanks even after a first failed print job was over 135 hours. Most AM processes require post process after part building to prepare the part for its intended form, fit and/or function. Depending on on the AM technique, the reasons and procedures for post processing varies, but the most common type of post processing in AM is support removal [3].

The support material used in the propulsion tank is a rigid structure which was designed and built to support, restrain and/or attach the part being built to the build platform as seen in Figure 4.1. For PBF processed the metal supports are often too strong to be removed by hand thus, the use of mills, bandsaws, cut off blades, wire EDM, and other metal cutting techniques are widely employed. After removing the support material the finished propulsion tank can be seen in Figure 4.2.

Due to the build orientation of the propulsion tank, some sections came out with flaws. Some surfaces were not finished or were porous and were filled in with welding by the manufacturer which can be seen in Figure 4.3. One of the holes that is used for hardware interface was partially missing due to a small gusset diameter. Each propulsion tank was made one after the other and the manufacturer were able to correct some of these flaw as seen in Figure 4.4.



Figure 4.1: AM propulsion tank with support structure



(a) Front View



(b) Top View



(c) Left Side View



(d) Right Side View

Figure 4.2: Four view of the propulsion tank

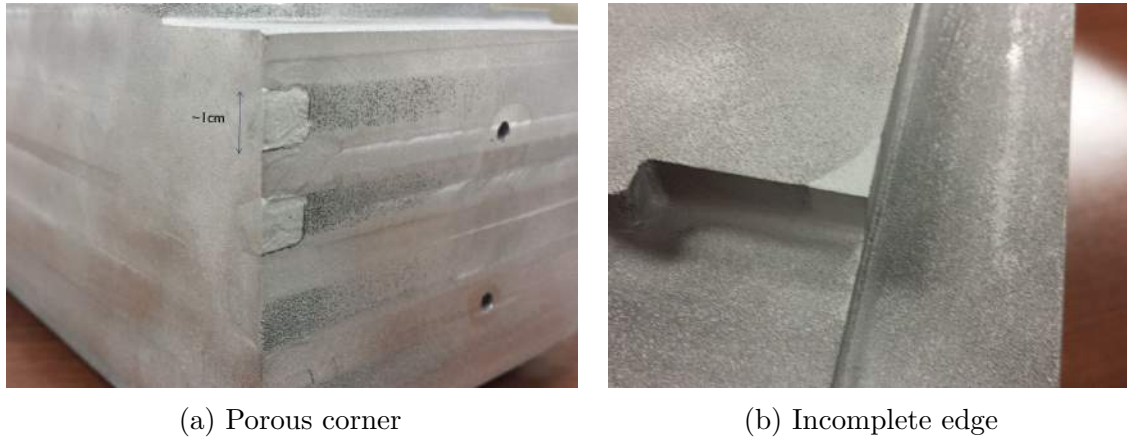


Figure 4.3: Flawed features



Figure 4.4: Flawed and corrected 1cm diameter hole

4.2 FEA Results

The FEA results show that the tank was over designed showing a minimum factor of safety of 2.1, a maximum displacement of .109mm, and a yield strength of $2.275e8 \text{ N/m}^2$ at 160psi which can be seen in Figures 4.5 and 4.6.

4.3 Propellant Tank Hydrostatic Pressure Test Results

The hydrostatic pressure test started with having the tank at it approximately it maximum design pressure of 160 psi and once that was achieved the pressure was

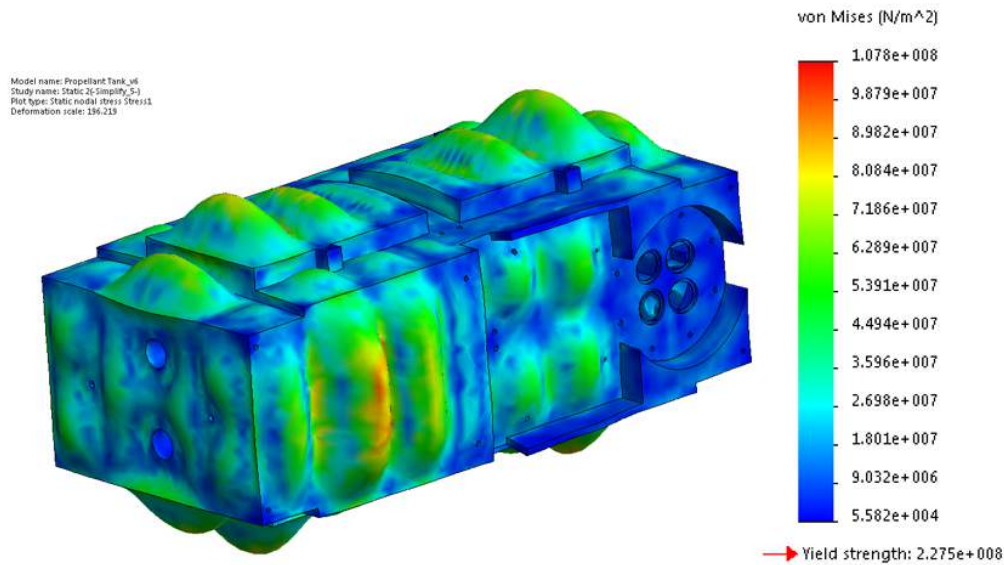


Figure 4.5: Von Mises Stress of the Propulsion Tank

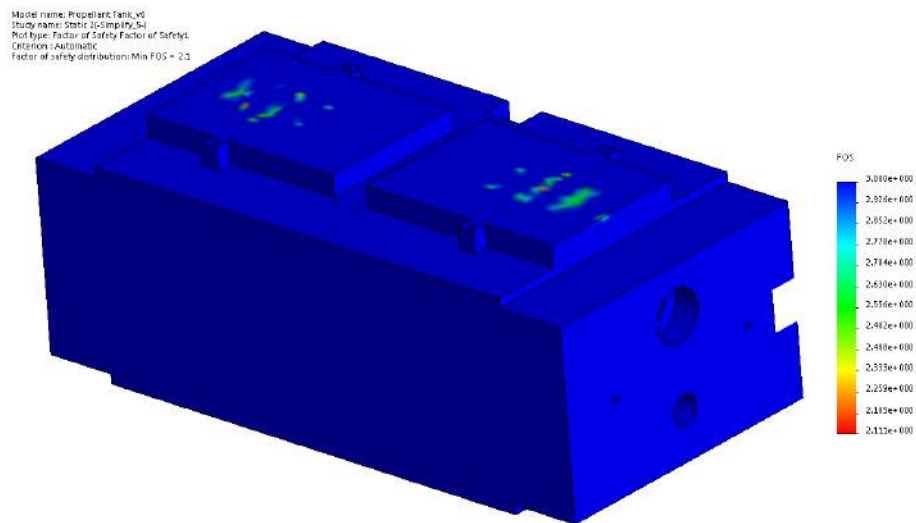


Figure 4.6: Factor of Safety of the Propulsion Tank

slowly ramped up until rupture which ended up being at approximately around 410 psi which can be seen in Figure 4.7.

Once opening the chamber, a misalignment in the hardware interface connections is clearly visible as seen in Figure 4.8. Removing the tank from the chamber you can clearly see a straight line next to the hardware interface connection where it ruptured which is shown in Figure 4.9.

Unfortunately, two of the six strain gages flat lined during the test and did not

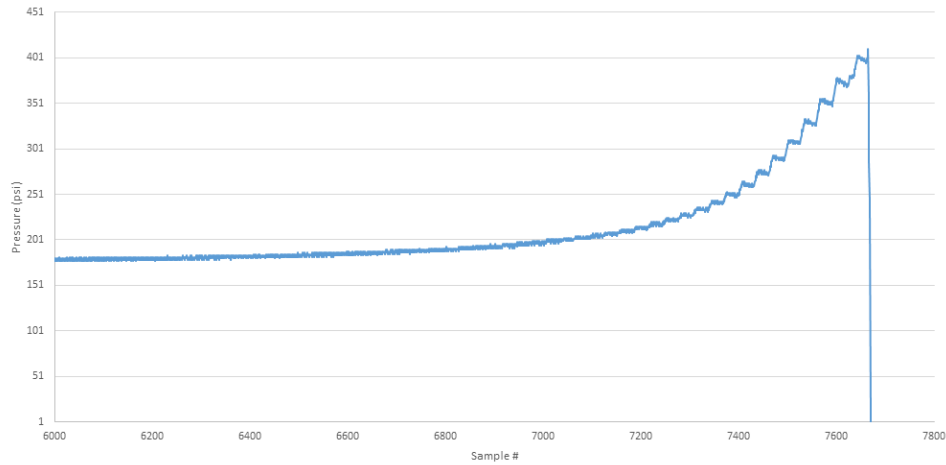
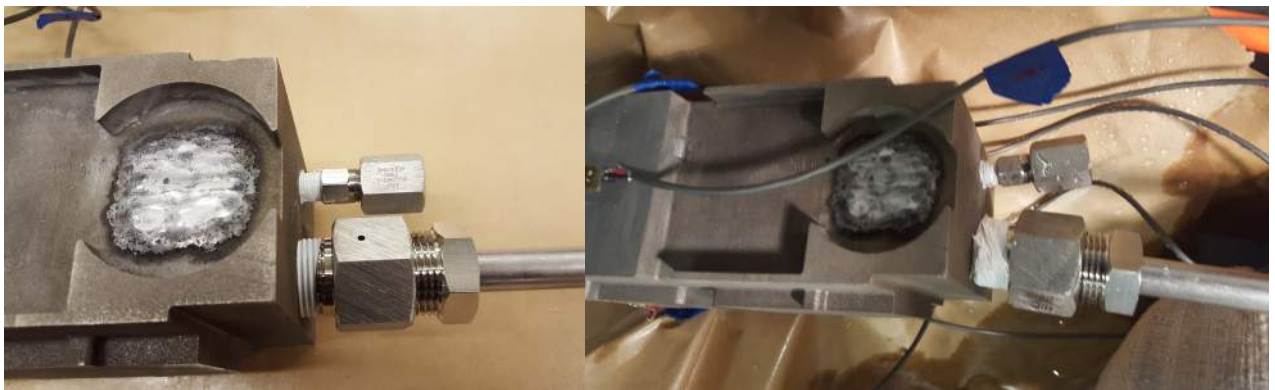


Figure 4.7: Internal pressure during testing



(a) Before Testing

(b) After Testing

Figure 4.8: Resulting connector displacement

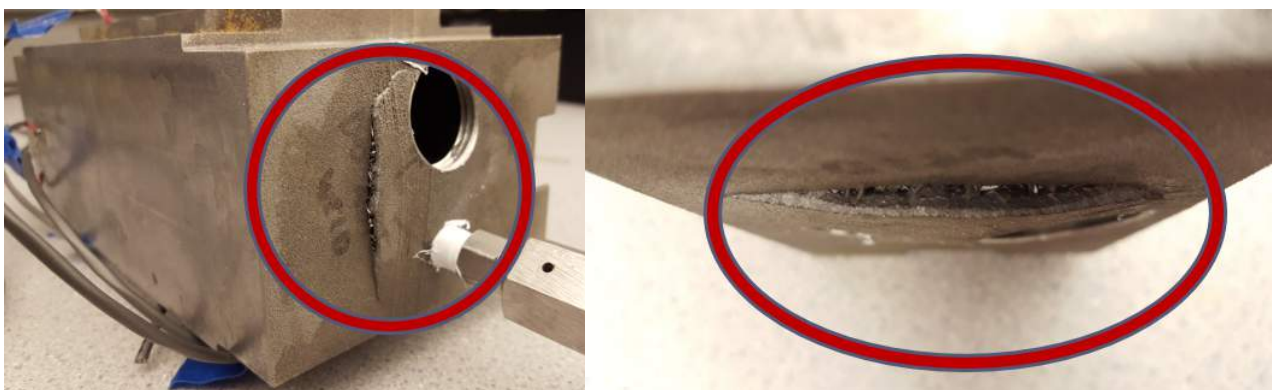


Figure 4.9: The rupture seam and close up

receive a signal at all and the remaining four did not record any usable data which will be discussed further in the following chapter.

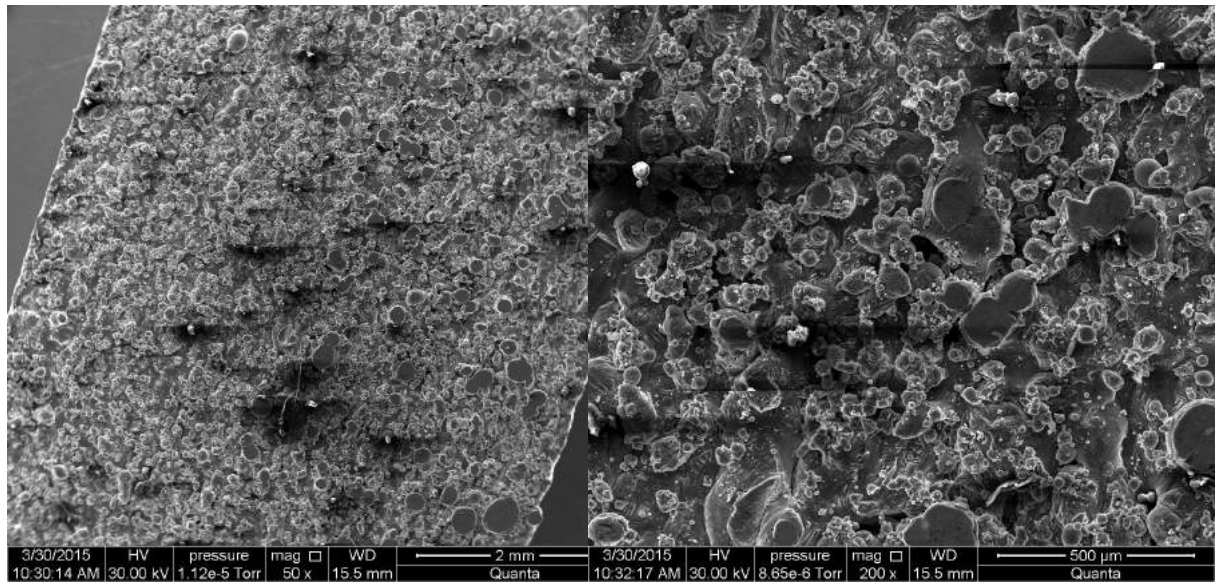
5 Discussion, Conclusion & Recommendations

5.1 Discussion

When installing the strain gages and bonding terminals, some porosity was encountered which reduced the amount of surface areas to be bonded to regardless of how much was sanded down and the grade of sandpaper which will affect the readings of the strain gages. A picture that was taken with the scanning electron microscope (SEM) can be seen in Figure 5.1 and you can see that the surface is not smooth but very porous compared to a part with a machine finish which is seen in Figure 5.2. More details of material properties that were gathered from the SEM can be seen in Appendix C.

Two strain gages were installed incorrectly due to this and were deemed unusable. The FEA study also showed that the maximum displacement with 160 psi of pressure would be 0.11 mm. The strain gages acquired were for general purpose and might have that high of sensitivity. So a smaller and more sensitive strain gage will have to be researched and purchased for future testing.

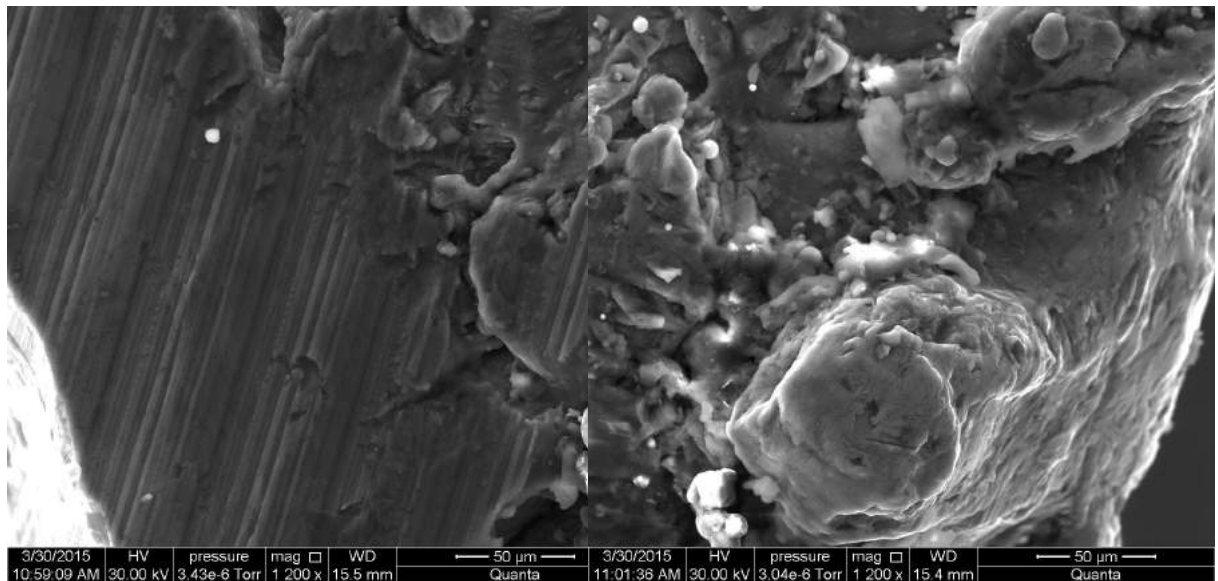
The team believes that the failure happened where it did next to the hardware interface device due to two reasons. The first being that the propulsion tank was cantilevered to the hydrostatic pressure system with just a sandbag simply supporting it in the downward direction at the other end and during the testing you can hear the diaphragm pump violently pumping water into the test subject. The team thinks that micro vibrations caused an increased stress at that location which is why



(a) 50x magnification

(b) 200x magnification

Figure 5.1: SEM pictures of the porous surface



(a) Machined Surface

(b) Porous AM Metal

Figure 5.2: 1200x magnification

it ruptured below the hardware interface device.

Second, once opening up the propulsion tank with a band saw we noticed that there was some irregularity with the material around the rupture but in the inside of the tank, which cannot be seen from the outside. This can be seen in Figure 5.3

and after closer examination it shows that the boss and gusset is not completely finished and you can spot some porosity in the material around the rupture also seen in Figure 5.4.



Figure 5.3: Unfinished boss and gusset

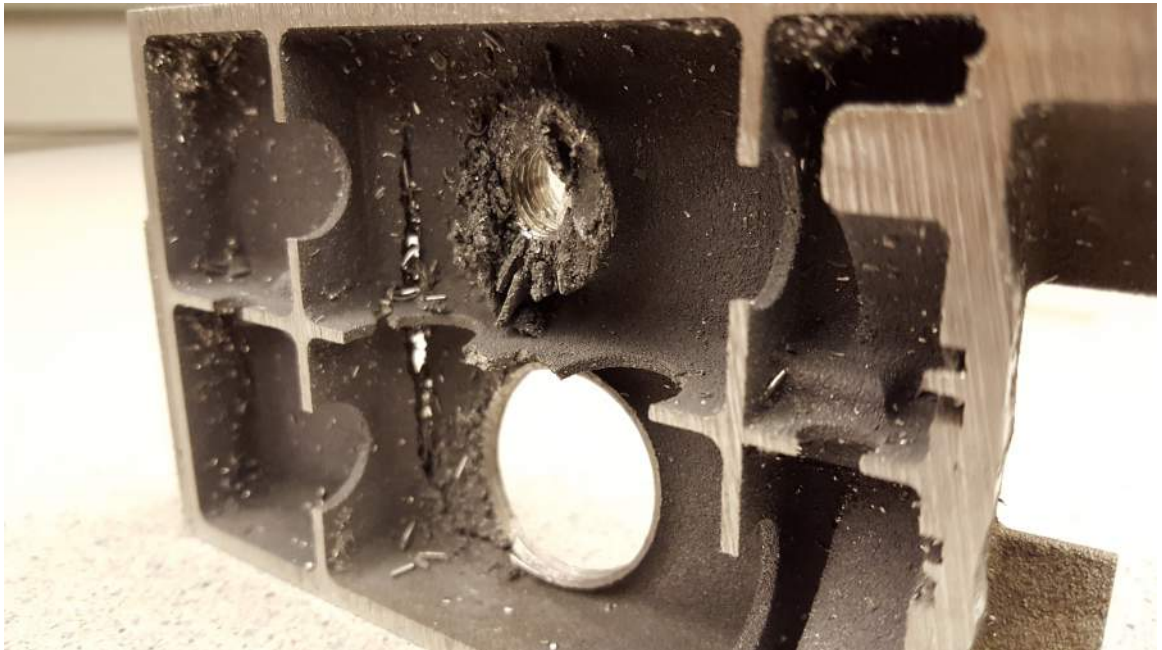


Figure 5.4: Visible material porosity around the rupture

5.2 Conclusion

Regardless of the lack of usable strain gage data, the pressure which the propulsion tank ruptured was approximately 2.5 times the operating pressure and the factor of safety that the FEA showed was 2.1 showing that the material properties of AlSi10Mg is slightly superior to Aluminum 6061 T6. The AM technology seemed to be a viable option to make pressure vessels, but more testing needs to be conducted in the future which is also explained in the next section.

5.3 Recommendations and Future Work

When designing the new iteration of the propulsion tank there are a number of recommendations that should be considered. The first one is to design for AM, not only to reduce the cost of manufacturing but to reduce the number of flaws that were presented in this current propulsion tank. The complexity of the internal baffles were added to test the limits of AM, but they were still designed to current design for manufacturing (DFM) and design for assembly (DFA) practices. The internal baffles can be designed to be lightweight and more organic, like a lattice structure. An example of such can be seen in Figure 5.5.

A second recommendation is to do a topography optimization study to reduce the number amount of baffles, vessel wall thicknesses, and mass while still meeting the required design criteria. A parametric optimization study was attempted to be performed but HEEDS MDO which is superior to Solidwork's Optimization toolbox, but the software licenses were not activated for the semester yet.

The manufacturer that made the two propulsion tanks also provided tensile test samples but unfortunately the tensile tester machine in the materials lab was out of order during the semester and the smaller machine in the structures lab does not

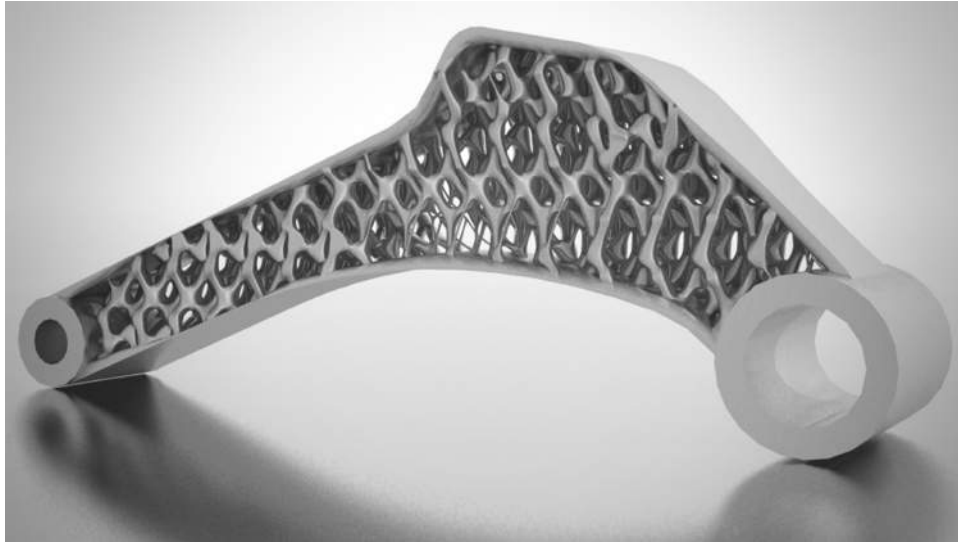


Figure 5.5: Exmaple of lattice structure as internal supports [2]

provide enough force to test the sample. When then machine is back in operation we can go and test the size sample.

5.4 Application

The application of this propulsion tank is the purpose of its development and testing. While this one was tested to failure, the second propulsion tank that was manufactured was sent to Dr. Adam Huang at the University of Arkansas to install all the remaining components like the inhibit valves, nozzles and electronic components. That propulsion tank will be a flight ready model with plans to be fully integrated in the ARAPAIMA cubesat which will undergo further testing, for example vibration testing, thermal bake out and radiation testing.

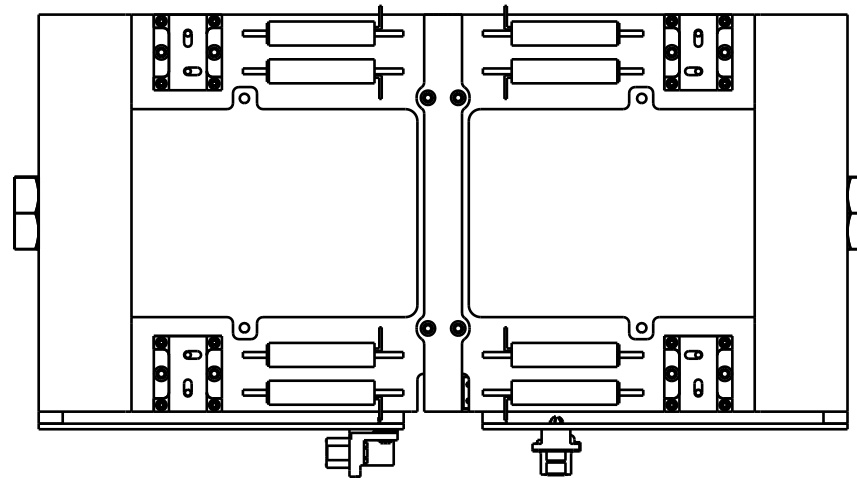
Bibliography

- [1] AFRL. *Nanosat-8 User's Guide*. Revision A. University NanoSat-8 Program. 2013.
- [2] Altaior. *Topography Optimization Methods*. URL: <http://www.altair.com/Default.aspx>.
- [3] Wolhers Associates. *Wolhers Report 2013*. Additive Manufacturing and 3D Printing States of Industry, Annual Worldwide Progress Report. 2013.
- [4] Planetary Systems Corporation. *Canisterized Satellite Dispenser*. URL: http://www.planetarysystemscorp.com/?post_type=product&p=448.
- [5] Rick Fletter. *The Logic of Microspace*. Technology Management of Minimum Cost Space Missions. 2000.
- [6] Peter Fortescue and John Stark. *Spacecraft Systems Engineering*. 2nd Edition. 1995.
- [7] Dongdong Gu. *Laser Additive Manufacturing of High-Performance Materials*. 2015.
- [8] Adam Huang. "UNP Propulsion Waiver". In: 2014.
- [9] David Rosen Ian Gibson and Brent Stucker. *Additive Manufacturing Technologies*. 2nd Edition. 3D Printing, Rapid Prototyping, and Direct Digital Manufacturing. 2015.
- [10] National Instruments. *How To Measure Pressure with Pressure Sensors*. URL: <http://www.ni.com/white-paper/3639/en/>.
- [11] National Instruments. *What is LabVIEW*. URL: <http://www.ni.com/newsletter/51141/en/>.
- [12] CubeSat Kit. *Begin your CubeSat Mission with the CubeSat Kit*. URL: <http://www.cubesatkit.com/>.
- [13] Andrew D. Ketsdever; Michael M. Micci. *Micropropulsion for Small Spacecraft*. Progress in Astronautics and Aeronautics. 2000.
- [14] Vishay Micro-Measurements. *Instruction Bulletin B-127-14*. 2014.
- [15] Omega. *Pressure Transducers*. URL: <http://www.omega.com/section/pressure-transducers.html>.
- [16] James F. Peters. *Spacecraft Systems Design and Operations*. Essential Subsystems for Manned and Unmanned Spacecraft. 2004.

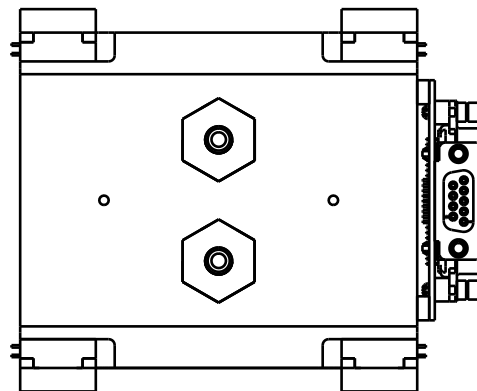
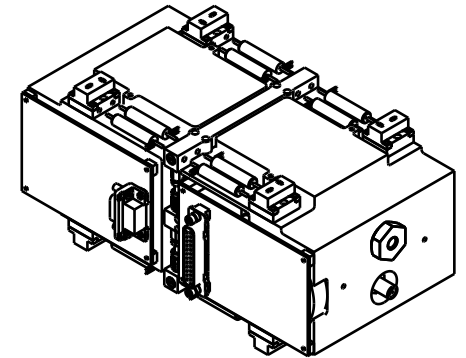
- [17] PolySat. *Poly- PicoSatellite Orbital Dispenser*. URL: <http://polysat.calpoly.edu/>.
- [18] ProtoLabs. *Design for DMLS*. URL: <http://www.protolabs.com/resources/design-tips>.
- [19] Abraham Warshavsky Shimshon Adler and Arie Peretz. “Low-Cost Cold-Gas Reaction Control System for Slosat FLEVO Small Satellite”. In: *Journal of Spacecraft and Rockets*. Vol. 42. 2. 2005, pp. 345–351.
- [20] Purvesh Thakker and Wayne Shiroma. *Emergence of Pico- and Nanosatellites for Atmospheric Research and Technology Testing*. Vol. 234. 2010.
- [21] Martin J.L. Turner. *Rocket and Spacecraft Propulsion*. 3rd Edition. Principles, Practices and New Developments. 2010.
- [22] Robert Twigg. “CubeSat Development in Education and into Industry”. In: *AIAA Space 2006 Conference*. 2006.
- [23] James R. Wertz and Wiley J. Larson. *Space Mission Analysis and Design*. 3rd Edition. 1999.

A Propulsion Tank Detailed Drawings

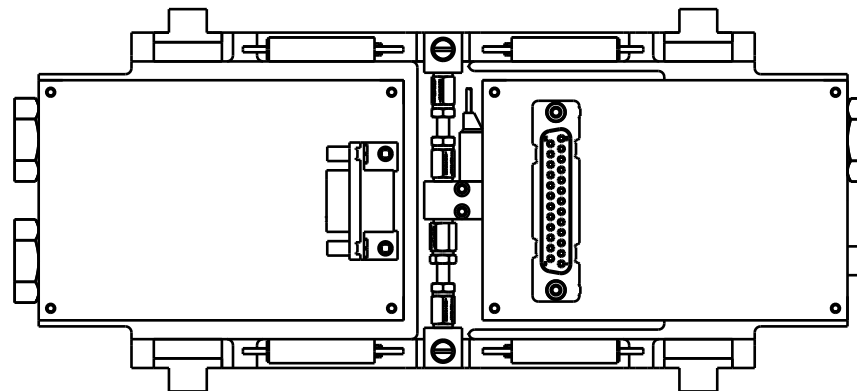
TOP VIEW



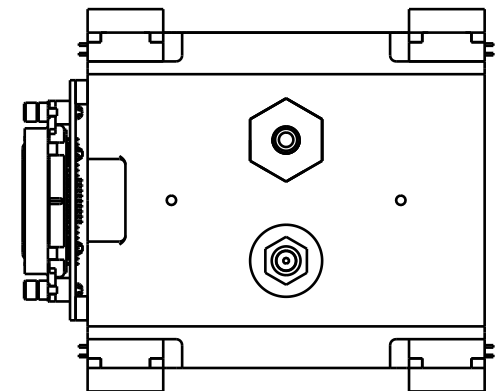
ISO VIEW



LEFT SIDE VIEW



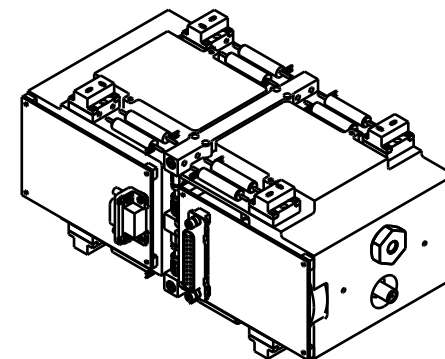
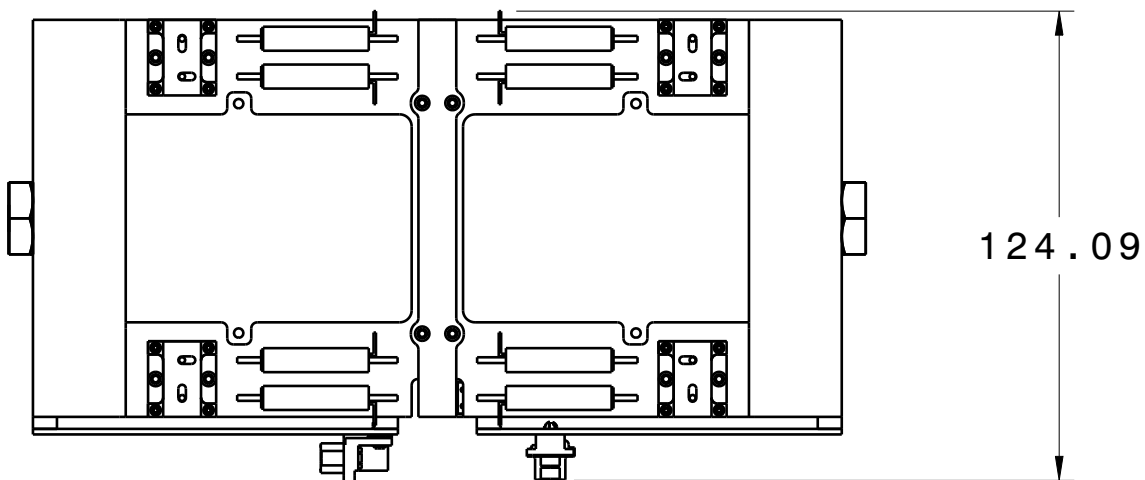
FRONT VIEW



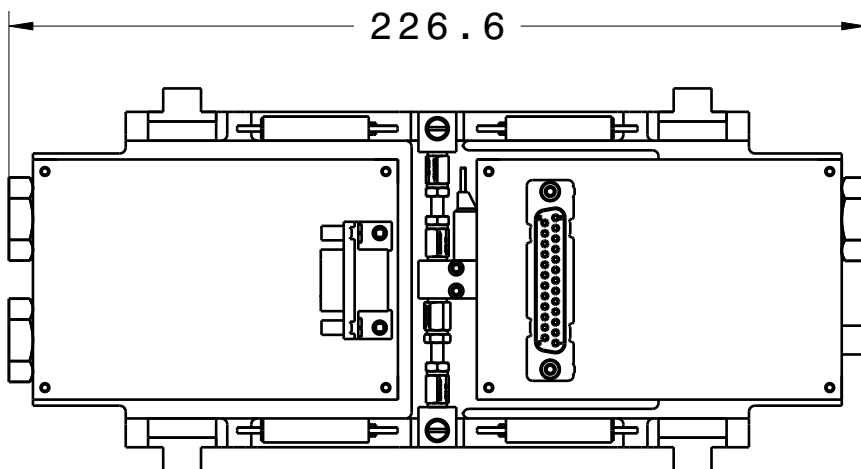
RIGHT SIDE VIEW

EMBRY RIDDLE AERONAUTICAL UNIVERSITY DAYTONA BEACH, FLORIDA			
SIZE: A	DATE: 9/29/15	SCALE: 1=2	CLASS SECTION: N/A
DRAWN BY: GEOVANNI SOLORZANO			
DRAWING TITLE: PROPELLANT TANK 5 VIEW			SHEET: 1 / 4

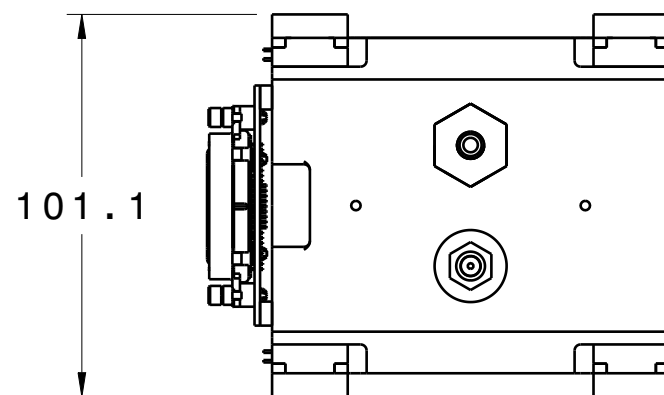
TOP VIEW



ISO VIEW

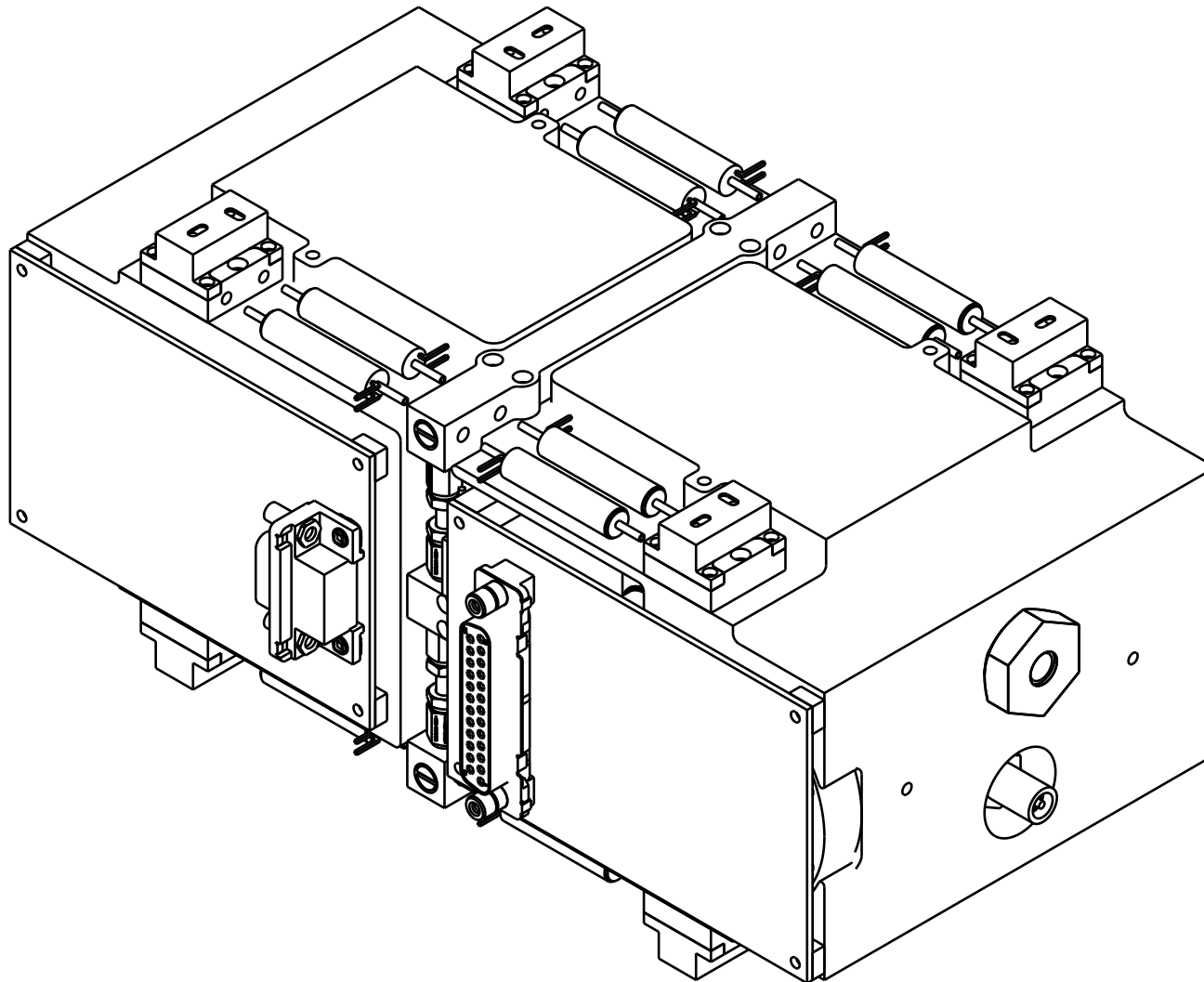


FRONT VIEW



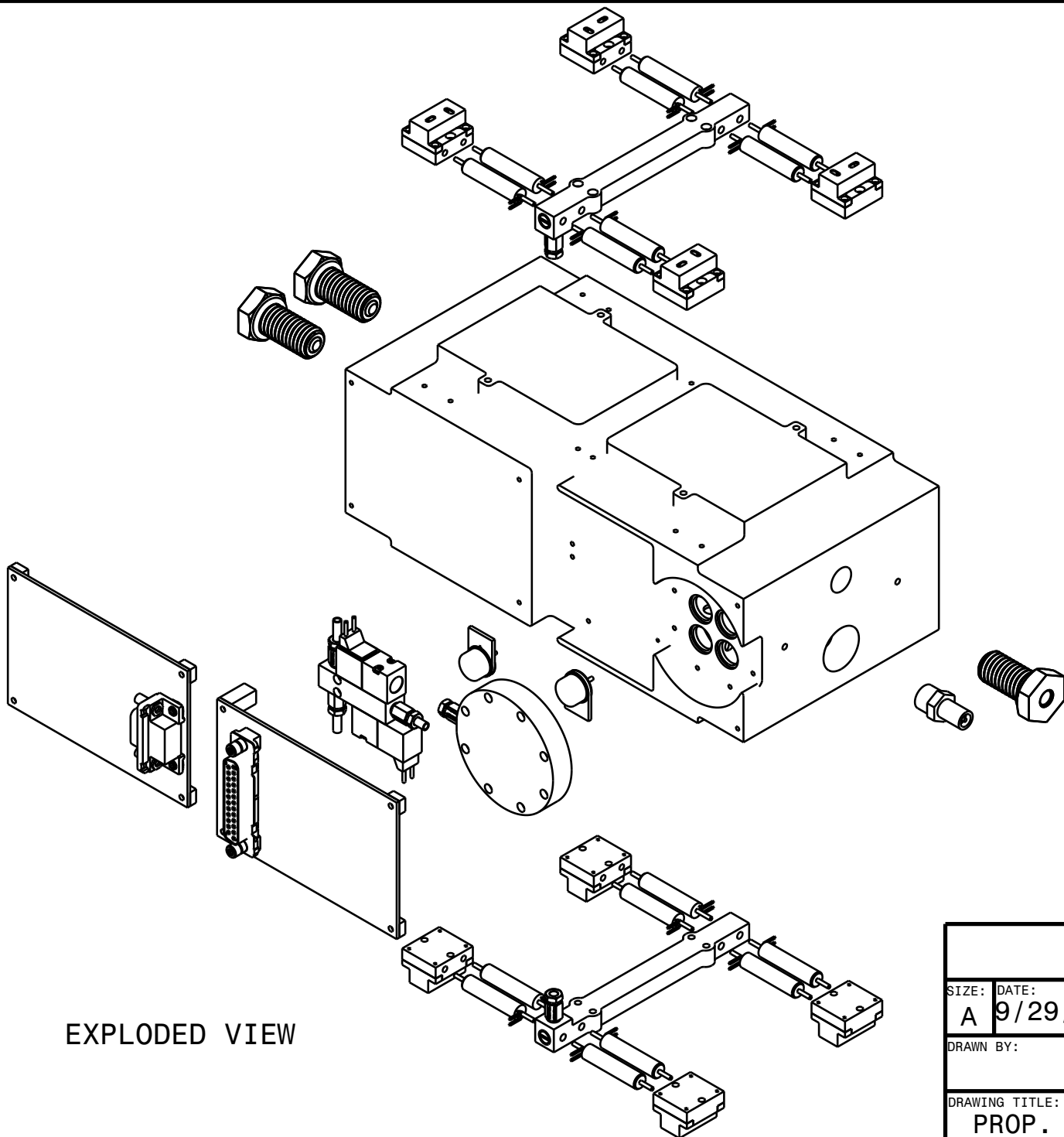
RIGHT SIDE VIEW

EMBRY RIDDLE AERONAUTICAL UNIVERSITY DAYTONA BEACH, FLORIDA			
SIZE: A	DATE: 9/29/15	SCALE: 1=2	CLASS SECTION: N/A
DRAWN BY: GEOVANNI SOLORIZANO			
DRAWING TITLE: PROPELLANT TANK 4 VIEW DIM			SHEET: 2/4



ISO VIEW

EMBRY RIDDLE AERONAUTICAL UNIVERSITY DAYTONA BEACH, FLORIDA			
SIZE: A	DATE: 9/29/15	SCALE: 3=4	CLASS SECTION: N/A
DRAWN BY: GEOVANNI SOLORIZANO			
DRAWING TITLE: PROPELLANT TANK ISO VIEW			SHEET: 4 / 4



EXPLODED VIEW

EMBRY RIDDLE AERONAUTICAL UNIVERSITY DAYTONA BEACH, FLORIDA			
SIZE: A	DATE: 9/29/15	SCALE: 9=20	CLASS SECTION: N/A
DRAWN BY: GEOVANNI SOLORZANO			
DRAWING TITLE: PROP. TANK EXPLODED VIEW			SHEET: 3/4

B EOS Aluminium AlSi10Mg Data Sheet

Material data sheet

EOS Aluminium AlSi10Mg

EOS Aluminium AlSi10Mg is an aluminium alloy in fine powder form which has been specially optimised for processing on EOSINT M systems

This document provides information and data for parts built using EOS Aluminium AlSi10Mg powder (EOS art.-no. 9011-0024) on the following system specifications:

- EOSINT M 280
with PSW 3.5 and Original EOS Parameter Set AlSi10Mg_Speed 1.0

Description

AlSi10Mg is a typical casting alloy with good casting properties and is typically used for cast parts with thin walls and complex geometry. It offers good strength, hardness and dynamic properties and is therefore also used for parts subject to high loads. Parts in EOS Aluminium AlSi10Mg are ideal for applications which require a combination of good thermal properties and low weight. They can be machined, spark-eroded, welded, micro shot-peened, polished and coated if required.

Conventionally cast components in this type of aluminium alloy are often heat treated to improve the mechanical properties, for example using the T6 cycle of solution annealing, quenching and age hardening. The laser-sintering process is characterized by extremely rapid melting and re-solidification. This produces a metallurgy and corresponding mechanical properties in the as-built condition which is similar to T6 heat-treated cast parts. Therefore such hardening heat treatments are not recommended for laser-sintered parts, but rather a stress relieving cycle of 2 hours at 300 °C (572 °F). Due to the layerwise building method, the parts have a certain anisotropy, which can be reduced or removed by appropriate heat treatment - see Technical Data for examples.

Material data sheet

Technical data

General process and geometrical data

Typical achievable part accuracy [1]	$\pm 100 \mu\text{m}$
Smallest wall thickness [2]	approx. 0.3 – 0.4 mm approx. 0.012 – 0.016 inch
Surface roughness, as built, cleaned [3]	R _a 6 – 10 μm , R _z 30 – 40 μm R _a 0.24 – 0.39 $\times 10^{-3}$ inch R _z 1.18 – 1.57 $\times 10^{-3}$ inch
- after micro shot-peening	R _a 7 – 10 μm , R _z 50 – 60 μm R _a 0.28 – 0.39 $\times 10^{-3}$ inch R _z 1.97 – 2.36 $\times 10^{-3}$ inch
Volume rate [4]	7.4 mm ³ /s (26.6 cm ³ /h) 1.6 in ³ /h

- [1] Based on users' experience of dimensional accuracy for typical geometries. Part accuracy is subject to appropriate data preparation and post-processing, in accordance with EOS training.
- [2] Mechanical stability dependent on the geometry (wall height etc.) and application
- [3] Due to the layerwise building, the surface structure depends strongly on the orientation of the surface, for example sloping and curved surfaces exhibit a stair-step effect. The values also depend on the measurement method used. The values quoted here given an indication of what can be expected for horizontal (up-facing) or vertical surfaces.
- [4] The volume rate is a measure of the building speed during laser exposure. The overall building speed is dependent on the average volume rate, the time required for coating (depends on the number of layers) and other factors, e.g. DMLS settings.

Material data sheet

Physical and chemical properties of the parts

Material composition	Al (balance) Si (9.0 – 11.0 wt-%) Fe (\leq 0.55 wt-%) Cu (\leq 0.05 wt-%) Mn (\leq 0.45 wt-%) Mg (0.2 – 0.45 wt-%) Ni (\leq 0.05 wt-%) Zn (\leq 0.10 wt-%) Pb (\leq 0.05 wt-%) Sn (\leq 0.05 wt-%) Ti (\leq 0.15 wt-%)
Relative density	approx. 100 %
Density	2.67 g/cm ³ 0.096 lb/in ³

Material data sheet

Mechanical properties of the parts

	As built	Heat treated [8]
Tensile strength [5]		
- in horizontal direction (XY)	430 ± 20 MPa 62.4 ± 2.9 ksi	425 ± 20 MPa 61.6 ± 2.9 ksi
- in vertical direction (Z)	430 ± 20 MPa 62.4 ± 2.9 ksi	420 ± 20 MPa 60.9 ± 2.9 ksi
Yield strength (Rp 0.2 %) [5]		
- in horizontal direction (XY)	245 ± 10 MPa 35.5 ± 1.5 ksi	275 ± 10 MPa 39.8 ± 1.5 ksi
- in vertical direction (Z)	220 ± 10 MPa 31.9 ± 1.5 ksi	250 ± 10 MPa 36.3 ± 1.5 ksi
Modulus of elasticity		
- in horizontal direction (XY)	approx. 70 ± 5 GPa approx. 10.2 ± 0.7 Msi	approx. 70 ± 5 GPa approx. 10.2 ± 0.7 Msi
- in vertical direction (Z)	approx. 65 ± 5 GPa approx. 9.4 ± 0.7 Msi	approx. 65 ± 5 GPa approx. 9.4 ± 0.7 Msi
Elongation at break [5]		
- in horizontal direction (XY)	(9.5 ± 2) %	(6 ± 2) %
- in vertical direction (Z)	(7.5 ± 2) %	(4 ± 2) %
Hardness [6]	120 ± 5 HBW	
Fatigue strength [7]		
- in vertical direction (Z)	97 ± 7 MPa 14.1 ± 1.0 ksi	

[5] Mechanical strength tested as per ISO 6892-1:2009 (B) annex D, proportional specimens, specimen diameter 5 mm, initial measured length 25 mm.

[6] Hardness test in accordance with Brinell (HBW 2.5/62.5) as per DIN EN ISO 6506-1. Note that measured hardness can vary significantly depending on how the specimen has been prepared.

[7] Fatigue test with test frequency of 50 Hz, R = -1, measurement stopped on reaching 5 million cycles without fracture.

[8] Stress relieve: anneal for 2 h at 300 °C (572 °F).

Material data sheet

Thermal properties of parts

	As built	Heat treated [8]
Thermal conductivity (at 20 °C)		
- in horizontal direction (XY)	approx. 103 ± 5 W/m °C	approx. 173 ± 10 W/m °C
- in vertical direction (Z)	approx. 119 ± 5 W/m °C	approx. 175 ± 10 W/m °C
Specific heat capacity		
- in horizontal direction (XY)	approx. 920 ± 50 J/kg°C	approx. 890 ± 50 J/kg°C
- in vertical direction (Z)	approx. 910 ± 50 J/kg°C	approx. 900 ± 50 J/kg°C

Abbreviations

approx. approximately
wt weight

Notes

The data are valid for the combinations of powder material, machine and parameter sets referred to on page 1, when used in accordance with the relevant Operating Instructions (including Installation Requirements and Maintenance) and Parameter Sheet. Part properties are measured using defined test procedures. Further details of the test procedures used by EOS are available on request.

The data correspond to our knowledge and experience at the time of publication. They do not on their own provide a sufficient basis for designing parts. Neither do they provide any agreement or guarantee about the specific properties of a part or the suitability of a part for a specific application. The producer or the purchaser of a part is responsible for checking the properties and the suitability of a part for a particular application. This also applies regarding any rights of protection as well as laws and regulations. The data are subject to change without notice as part of EOS' continuous development and improvement processes.

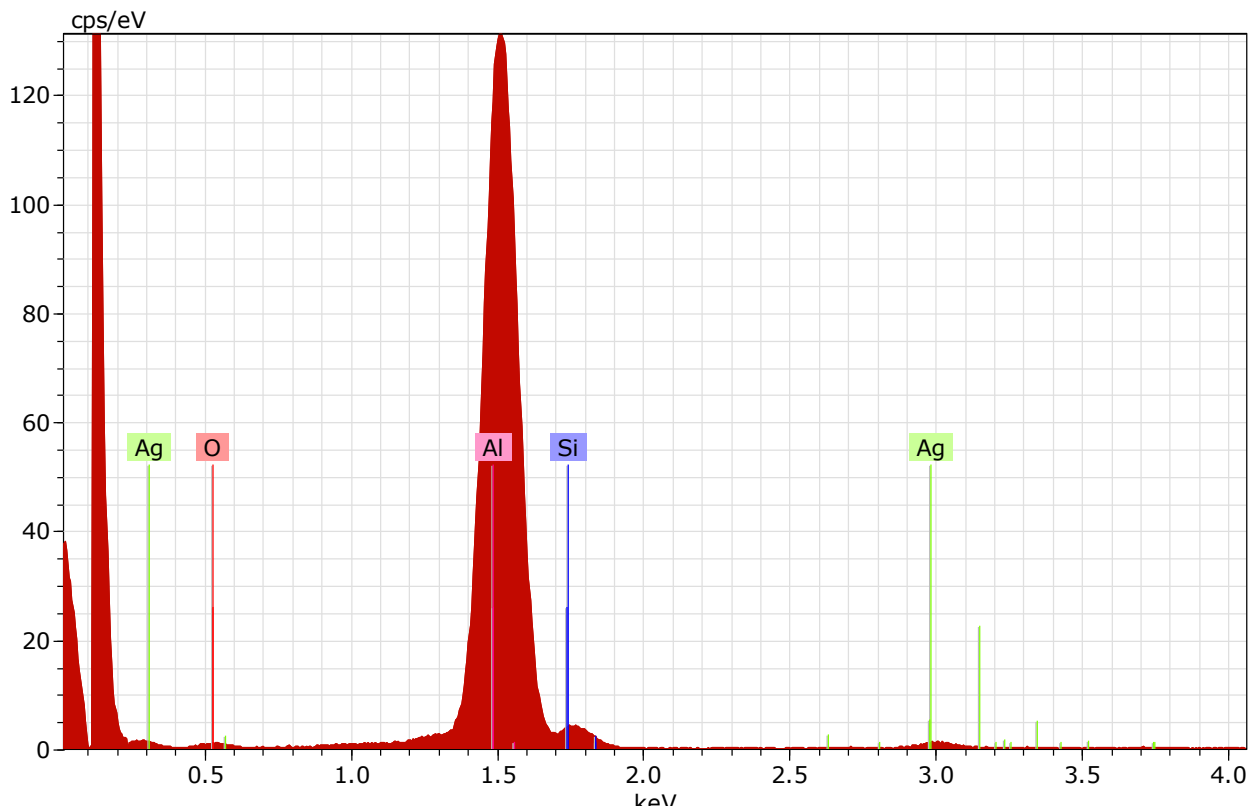
EOS®, EOSINT® and DMLS® are registered trademarks of EOS GmbH.

© 2011 EOS GmbH – Electro Optical Systems. All rights reserved.

C SEM Material Test Sample Results

Application Note

Company / Department



Spectrum: Test

El	AN	Series	Net	unn. C	norm. C	Atom. C	Error (1 Sigma)
			[wt.%]	[wt.%]	[wt.%]	[at.%]	[wt.%]
Al	13	K-series	369852	67.49	77.51	74.70	3.41
Si	14	K-series	15829	9.76	11.20	10.37	0.47
O	8	K-series	3002	7.68	8.82	14.33	1.35
Ag	47	L-series	4024	2.15	2.47	0.60	0.10
Total:			87.08	100.00	100.00		

